MARMARA UNIVERSITY

INSTITUTE FOR GRADUATE STUDIES

IN PURE AND APPLIED SCIENCES

NUMERICAL ANALYSIS OF HYDRODYNAMICS IN A PRESSURIZED CIRCULATING FLUIDIZED BED SYSTEM

MİLAD ANSARLAR

MASTER THESIS

Department of Mechanical Engineering

Thesis Supervisor

Prof.BARIS YILMAZ

ISTANBUL, 2023

Table of Contents

Table of Figures

NOMENCLATURE

ω	
τ_p	stress tensor
τ_f	viscous stress
θ_p	volume fraction
θ_f	volume fraction
θ_{cp}	close pack volume fraction
ε	Volume fraction.
β	Interphase momentum transfer coefficient
u_p	velocity
u_f	gas velocity
p	pressure
m_p	particle mass
g	gravity
Vp	volume of the particle
P_s	Pressure
F	body force
D_p	drag function.
C_d	drag coefficient
Ψ	Sphericity
τ_p	particle normal stress
Re	Reynolds number
D_V	Volume diameter
D_{SV}	Surface Volume diameter
D_P	Sieve size
D	drag function
μ	Viscosity
€	voidage
U_{mf}	Minimum fluidization velocity
ε_{mf}	Minimum fluidization Volume fraction

ABBREVIATIONS

Mbarg :	Milibar Gage
Mtoe :	Million Tons Oil Equivalent
CFB :	Circulated Fluidized Bed
BFB :	Bubbling Fluidized Bed
CFD :	Computational Fluid Dynamics
SO_2 :	Sulfur Dioxide
NO_x :	Nitrogen oxides
PFBC :	Pressurised Fluidized Bed Combustion
AFBC :	Atmospheric Fluidized Bed Combustion
CPFD :	Computational Particle Fluid Dynamics
LES :	Large Eddy Simulation
MFC :	Mass Flow Controller

ÖZET

BASINÇLI BİR DOLAŞIMLI AKIŞKAN YATAK SİSTEMİNDE HİDRODİNAMİĞİN SAYISAL ANALİZİ

Küresel enerji talebinin gelecek yıllarda da artacağı ve tüm dünyada güç santrali sayısının artmaya devam edeceği görülmektedir. Buna bağlı olarak fosil yakıtların kullanımı da tüm dünyada artmaktadır. İstatistiklere göre bu talep her yıl bir önceki yıla göre artış göstermektedir. Diğer yandan, küresel ısınma insanlığın günümüzde en önemli sorunlarından birisidir ve küresel ısınmanın en önemli sorumlularından olan fosil yakıtlar, sera gazı salımlarının en önemli kaynağıdır. Enerjiye olan ihtiyaç nedeniyle güç santrallerinin sayısını azaltmak veya üretimini düşürmek mümkün değildir. Ancak bu santrallerin oluşturduğu kirlilik miktarı, verimlerinin arttırılması ile azaltılabilir. Bu alanda son yıllarda birçok araştırma ve çalışmalar yapılmaktadır. Günümüzde bilgisayar teknolojinin ilerlemesi sayesinde hesaplama süresi ve yüksek maliyetinden dolayı araştırılması mümkün olmayan yanma işlemi bugün farklı yönleriyle araştırılabilmektedir. Sayısal modelleme çalışmaları ve analizler, araştırmacılara karmaşık işlemler üzerinde çalışmalarına olanak sağlamaktadır. Böylece, sayısal modelleme yöntemi ile deneysel yöntemlerle zor ve pahalı olan ölçümler yapılabilmekte ve sistemler tasarlanamaktadır. Diğer yandan, simülasyonlarla elde edilmiş sonuçların laboratuvar verileri ile doğrulanması, yanma işlemlerinin geliştirilmesi ve araştırılmasında önemlidir.

Bu tez çalışmasında, laboratuvar verisinin ve yanma teorilerinin incelenmesiyle basınçlı bir Dolaşımlı Akışkan Yatak Sistemi sayısal olarak incelenecektir. Bu analizler sonucunda, akışkan yatak reaktöründe yanma verimini arttırmak ve çalışma parametrelerinin etkileri detaylı olarak incelenecektir. Geliştirilecek sayısal model ileride yapılacak boyut yükseltme çalışmalarında da kullanılabilir.

ABSTRACT

NUMERICAL ANALYSIS OF HYDRODYNAMICS IN A PRESSURIZED CIRCULATING FLUIDIZED BED SYSTEM

The global energy demand is predicted to increase in the coming decades. And every year the number of power plants around the world is increasing. Besides, the use of fossil fuels in the world is increasing, and the statistics show that this demand has increased every year compared to last year. On the other hand, environmental pollution is one of the main concerns of humans, and fossil fuels are one of the main sources of greenhouse gas emissions. It is not possible to reduce the number of power plants or reduce their production at the moment. However, the amount of pollution they produce can be decreased by increasing their efficiency, which requires a more detailed analysis of the processes taking place inside these power plants. Although studies and researches have been done in this field in the past years, today, thanks to the advancement of technology, the combustion process can be studied from other aspects, which were not possible before due to computational time and high cost. Numerical studies and analysis can greatly help researchers to study the complex processes so that they can not only use it to better understand the process, but also explore aspects of process behavior that may not have been possible before in experimental models. On the other hand, what is important is to ensure that the simulated model is well developed to represent the real laboratory model. Therefore, it can be said that verifying laboratory data with corresponding simulation models plays an important role in improving and investigating the combustion process. In this study, we will try to obtain the closest simulation model by examining laboratory data and combustion theories so that we can rely on the results to evaluate the effective parameters to increase the output efficiency of the fluidized bed-chamber. The developed model can be also used for further scale-up studies.

1 INTRODUCTION

1.1 Global Energy Profile

The supply of fossil propellants, like oil and coal are continuing to decrease at an equally rapid rate, while at the same time, the demand for energy is continuing to rise at a rapid rate as a result of increasing population and economic development. Currently, a considerable amount of the primary energy consumption that occurs on a global scale is attributable to the usage of fossil fuels. 12150 Mtoe were needed to meet global demand, with 32.8 percent coming from oil, 27.2 percent from coal, 20.9 percent from natural gas, 10.2 percent from biofuels and wastes, 5.8 percent from nuclear, 2.3 percent from hydropower, and 0.8 percent from other kinds of renewable energy [1]. Transportation, the generation of electricity, applications in industry, and even residential settings are some of the most common and widespread uses of these energy sources. These energy sources are put to use in a wide variety of contexts and settings.

It is estimated that approximately 31.7 percent of all primary energy sources that are utilised on a global scale come from the process of generating electricity [2]. Peat and coal accounted for 40.6 percent of the resources that were used in the production of electricity. This was followed by natural gas, which accounted for 21.4 percent of the resources, hydraulic power, which accounted for 16.2 percent, nuclear power, which accounted for 13.4 percent, oil, which accounted for 5.1 percent, and other forms of renewable energy, which accounted for 3.3 percent. Conventional combustion processes were responsible for the generation of the vast majority of the power, and these processes drew their fuel supplies from either solid fuels or gas fuels, depending on the nature of the process they were carrying out. As a result of this, people are consistently looking for ways to advance the traditional procedure or investigating new conversion technologies to achieve higher renovation efficiencies. This is done in order to meet the demand for increased conversion efficiencies.

The supply of primary energy in Turkey is broken down into the following categories according to the resources that feed it: 31.1 percent of the energy comes from coal and lignite, 28.8 percent from oil, 30.9 percent from natural gas, 4.4 percent from biofuels and wastes, 2.9 percent from hydropower, and 1.7 percent from other types of renewable energy foundations. Turkey had a main energy supply of 106 Mtoe, which is equivalent to 0.9 percent of the main energy source of the

entire world. The generation of electricity makes use of a proportion of the world's primary energy sources that is roughly equivalent to the consumption level seen on an everyday basis everywhere else in the world [3]. This number is 31.7 percent of the total. In terms of the proportion, this corresponds to 35.3% of Turkey's primary energy supply.

In Turkey, Natural gas is responsible for the generation of 50.1% of the electricity production, while coal and peat are responsible for 37.2% of electrical output, hydraulic power is responsible for 8.2% of electrical output, oil is responsible for 3.1% of electrical output, and renewable energy is responsible for 1.4% of electrical output. The vast majority of the nation's electricity, which is typically supplied by other countries, is produced through the utilisation of natural gas as a source of fuel. This results in the importation of electricity. Even though coal is the most important source of primary energy, it is only the second most important source of electricity generation that is primarily derived from domestic resources.

The use of coal in the energy industry is likely to remain significant for the foreseeable future and will likely continue to play an important role. Globally and domestically in Turkey, the demand for primary energy and the production of electricity places a substantial premium on the use of solid fuels such as coal and biomass. This holds true for both the production of electricity and the production of primary energy.

The current estimate for the total recoverable coal reserves across the globe is 948 billion tonnes, which, based on production rates across the globe, equates to a reserve to production ratio of 126 years. This estimate was developed using data collected from across the globe. This estimate was formulated using data gathered from various locations all over the world. The vast majority of those reserves are composed of anthracite and bituminous coal, which accounts for 47 percent of the total, sub-bituminous coal, which accounts for 30 percent of the total, and lignite reserves, which accounts for 23 percent of the total [4].

Although Turkey does not have a significant amount of oil or gas reserves, the country does have a sizeable amount of natural gas and coal reserves. It is estimated that Turkey in its current form has total recoverable coal reserves that amount to 14.6 billion tonnes, which is equivalent to 1.5 percent of the world's total coal reserves. These estimates are based on the country's historical coal production. According to this estimation, there are a combined 13.5 billion tonnes of lignite and 1.3 billion tonnes of hard coal. According to the production rates [5], the reserve to production

ratio for coal was calculated to be 171 years. It was determined that there were 171 years worth of reserves for every year of production, and the annual rate of total coal production was 85.3 million tonnes. This total is made up almost entirely of lignite, which is responsible for 84 million tonnes of the total weight.

In addition to Turkey's vast coal reserves, the country's biomass resources also have a significant amount of untapped potential as a national source of renewable energy that is derived from the waste products of forestry and agriculture. This type of energy can be produced by burning the residues that are left over from these industries. This opportunity arises from the fact that the country's biomass resources consist of organic matter that has been discarded by these two types of businesses. On an annual basis, it is estimated that Turkey's biomass resources have the potential to produce 32 Mtoe of energy. It is estimated that the annual economic recovery of biomass is approximately 17 Mtoe (Mtoe is an abbreviation for the term million tonnes of energy equivalent). Turkey consumed a total of 4.8 million tonnes of biomass per year. The energy that is stored in biomass can be reclaimed through the use of agricultural practises and waste, as well as residues from forestry and wood processing, municipal waste, and agricultural waste. This energy can also be recovered from municipal waste and agricultural waste. Domestic applications account for the vast majority of this product's consumption in more rural areas [6]. In particular, it is used in the kitchen and for heating homes.

Because of the world's coal reserves and the potential of biomass, the development of technologies for the conversion of solid fuels is taking on an increasing amount of significance both internationally and domestically in Turkey. This is the case in Turkey because of Turkey's position as a regional leader in this field. Numerous factors contribute to why this is the case. Finding a way to convert the dense fuel into the desired form (chemicals, electricity, artificial fuels, and others) that is as gentle as probable on the environment and as cost-effective as possible is the challenge that lies ahead. This is the challenge that needs to be overcome. It is possible to accomplish this goal through the application of a wide range of conversion technologies, some of which are already well-established, some of which are currently undergoing development, and some of which are on the verge of being commercialised. While some of these conversion technologies are already quite mature, others are still in the early stages of research and development.

Despite being the most readily available fuel source, coal is also the most significant contributor to the rise in CO2 emissions. Emissions of carbon dioxide are by far the most significant contributor to emissions of greenhouse gases. In addition, coal is the source of emissions of harmful gases such as sulphur dioxide, carbon monoxide, and nitrogen dioxide. In addition, the majority of the blame for the rising levels of carbon dioxide in the atmosphere can be placed at the feet of power plants that burn coal as their primary fuel source. Because of this, it is essential to implement technologies that are not only more effective but also cause less damage to the surrounding environment in order to lessen the negative effects that were outlined earlier. Pulverized and fluidized beds[7] are the two methods of coal combustion that are utilised today on the majority of the world's coal plants. In addition, pulverised methods are utilised. When utilising fluidized bed combustion, it is more important to reduce the negative effects brought on by the emissions produced by the combustion process than it is to reduce the emissions themselves. This is because fluidized bed combustion produces fewer emissions overall than other combustion methods. Oxy-fuel combustion has been the subject of a significant amount of research over the past few decades, specifically with regard to the possibility of burning coal more effectively and successfully capturing carbon dioxide [2–5]. This line of inquiry has been the focus of the majority of this investigation. Over the course of the last few decades, a significant amount of attention has been concentrated on pursuing this particular line of inquiry.

Utilizing fluidized bed reactors containing oxygen-rich atmospheres, this method permits the combustion of coal in either an atmosphere or a high-pressure environment. These conditions can both be satisfied. Fluidized bed combustion under oxyfuel conditions has been argued to hold the most promise as a technology for capturing and storing carbon. This is because of the conditions under which it operates. Because using this method already results in the flue gases being in a pressurised state, it is not necessary to use a compressor to pressurise the flue gases as a result of using this method. This is because using this method already results in the flue gases being in a pressurised state. Fluidized bed technology is frequently utilised for a wide variety of applications, including carbon capture and storage as well as clean coal combustion [8]. In order to accurately predict the emission levels and achieve the optimal working conditions for these highly dynamic systems, it is necessary to understand and optimise the gas-solid mixed-flow characteristics of the reactor as well as the interactions between these characteristics. In addition to this, it is necessary

to understand the relationships between these characteristics and to optimise those relationships. [9,10]

Scientists are currently conducting research on the flow characteristics of fluidized beds in an effort to gain a more in-depth understanding of the subject matter. Their goal is to gain a better grasp on the subject as a whole. Fluidized beds' hydrodynamic behaviour is influenced by a number of parameters, including the minimum fluidization velocity, the particle size distribution, the gas hold up, and the static bed height, amongst others. One of these parameters is the minimum fluidization velocity. An additional factor to take into consideration is the gas hold-up. Experiments are one method that can be used to investigate particle-flow interactions; however, these investigations are labor- and resource-intensive, particularly for large-scale facilities. Another method that can be used to investigate particle-flow interactions is computational modeling. Thanks to recent advancements in computing power and modeling techniques, numerical simulations are now capable of providing more comprehensive descriptions of hydrodynamic processes [11]. Because of these advancements, numerical simulations can now provide significantly more accurate predictions regarding the behavior of hydrodynamic systems.

1.2 **Aim of the study**

Different potential methods for carbon capture and storage can be used to reduce carbon dioxide emissions and cut down on carbon dioxide emissions. To increase the efficiency and capture carbon there are factors to take into account like the level of pressure, flow rate, and the quantity of oxygen. To find the best combination it is necessary to take all these parameters into account and change these variables and do the experiment over and over. Though, it is an expensive endeavor to continue investigating these challenges, both in terms of time and money. However, it would be possible to save both of these resources if, rather than experimenting, an accurate simulated example was created. The research presented in this thesis will include a numerical investigation of a laboratory-scale pressurized fluidized bed system’s cold flow riser analysis. The findings of this inquiry are going to be presented as the purpose of the research. Verifying that the output solutions of the simulated model are accurate is a prerequisite to employing the model in a practical setting. This investigation will focus on constructing a numerical model of a pressurized

CFB system's riser to assess the accuracy of the simulated mode by comparing it to data from prior studies. The data collected from these earlier trials will be utilized to confirm the simulation mode's dependability. This inquiry is being conducted in its totality to validate the dependability of the simulated mode. And finally, the pressure differences will be calculated at different pressure and temperatures.

1.3 BACKGROUND AND LITERATURE REVIEW

1.3.1 Technologies for Fluidized Bed Combustion

The transformation of solid particles that are inert into fluid-like properties is referred to as "fluidization," and it can be thought of as a transformation of fluid-like properties into fluid properties. This process is also known as a transformation of fluid-like properties into fluid properties. When solid particles are brought into contact with gas or liquid at a velocity that is high enough to be considered critical, this transformation can take place. This velocity must be high enough to be considered critical. Fluidized Bed Combustion is a cutting-edge technology that can burn fuels that have high levels of ash and moisture as well as low levels of calorific value. This is made possible by the fluidization of the bed in which the fuel is combusted. The fluidization of the bed in which the fuel is burned makes it possible for this to occur. The term "combustion" can also be referred to by its alternative moniker, "fluidized bed combustion," which is abbreviated as "FBC." The FBC is equipped with the capability to burn a wide variety of low-grade solid fuels such as coal, coke, and plastic, in addition to a wide variety of biomasses, with a high level of efficiency[12]. This ability is one of the FBC's most advantageous features. The fact that the FBC is capable of using a variety of fuels makes this possible. This is accomplished without the need for fuel preparation processes such as pulverization, which are necessary for other combustion systems to achieve the same results [13]. This can be accomplished without utilizing these processes. The use of limestone, which is used for sulphate flocculation, reduces the amount of sulphur emissions that are in the form of SO_2. As a consequence of this, the FBC is better able to meet its goal of reducing the number of emissions that it produces. In addition to this, the utilisation of FBC leads to a lower output of NO_x in comparison to what would occur in the event that it were not utilised, which results in a win for everyone involved. the primary reason for this is that the

temperatures at which combustion occurs are noticeably lower than those that are seen in traditional power plants. On the other hand, because of the lower temperatures, there have not been any problems with the ash melting in the FBC [14]. This is a direct result of the lower temperatures. Figure 1.1 provides a visual representation of the numerous kinds of fuel that were utilised in the FBC, along with the net calorific values that are associated with each kind of fuel. The following are examples of what these fuels were composed of: The illustration makes it abundantly clear that the difficulties that arise during the process of burning the fuel are significantly more manageable on the right side of the graph, whereas on the left side of the graph, they become progressively more difficult over time. This is the case because of the right side of the graph is located above the left side of the graph. The fossil fuels that are compatible with FBC are shown in the portion of the figure that is located to the right. On the other hand, applications on the left that involve municipal solid waste (MSW), RDF, and plastics present challenges for FBC. It is possible for the amount of thermal power required for combustion to range anywhere from 30 MWth to 90 MWth when using fluidized bed processes; however, in most cases, they will fall somewhere in the middle of that spectrum. In addition, the gasification process necessitates the utilisation of somewhere in the range of 8 to 10 MWth of power in order to be successful [15]. FBCs are utilised in thermal power ranges that are significantly higher the vast majority of the time. In addition to this, they are capable of functioning across an extremely extensive range of conceivable scenarios. Additionally, the production of NO_x that is caused by FBC is noticeably lower than that which is caused by other methods. This is due to the fact that FBC is a more efficient method. primarily because the temperatures at which the combustion takes place are noticeably lower than those that are found in traditional power plants. On the other hand, because of the lower temperatures in the FBC, there are no issues whatsoever with the ash melting [16]. Also included in this figure is an explanation of how the FBC was constructed. On the right side of the figure, the challenges that need to be conquered while the fuel is being burned are depicted as being less severe, while on the left side of the figure, the challenges that need to be conquered are depicted as being more severe. In order to accomplish the goals that have been set for the FBC process, it is possible to make use of the fossil fuels that are displayed on the right-hand side of the diagram. On the other hand, FBC applications that involve plastics, RDF, and municipal solid waste are faced with challenges. The wide range of power is necessary to ensure that the combustion process is successful. This is due to the highly variable amount of heat that is produced as a result of the combustion process.

Because of their versatility, FBCs are used in almost any situation in which an application requires a greater amount of thermal power. This is because FBCs are able to meet almost any demand. In addition to this, they are able to function within a very large parameter space that contains a variety of possible operational settings.

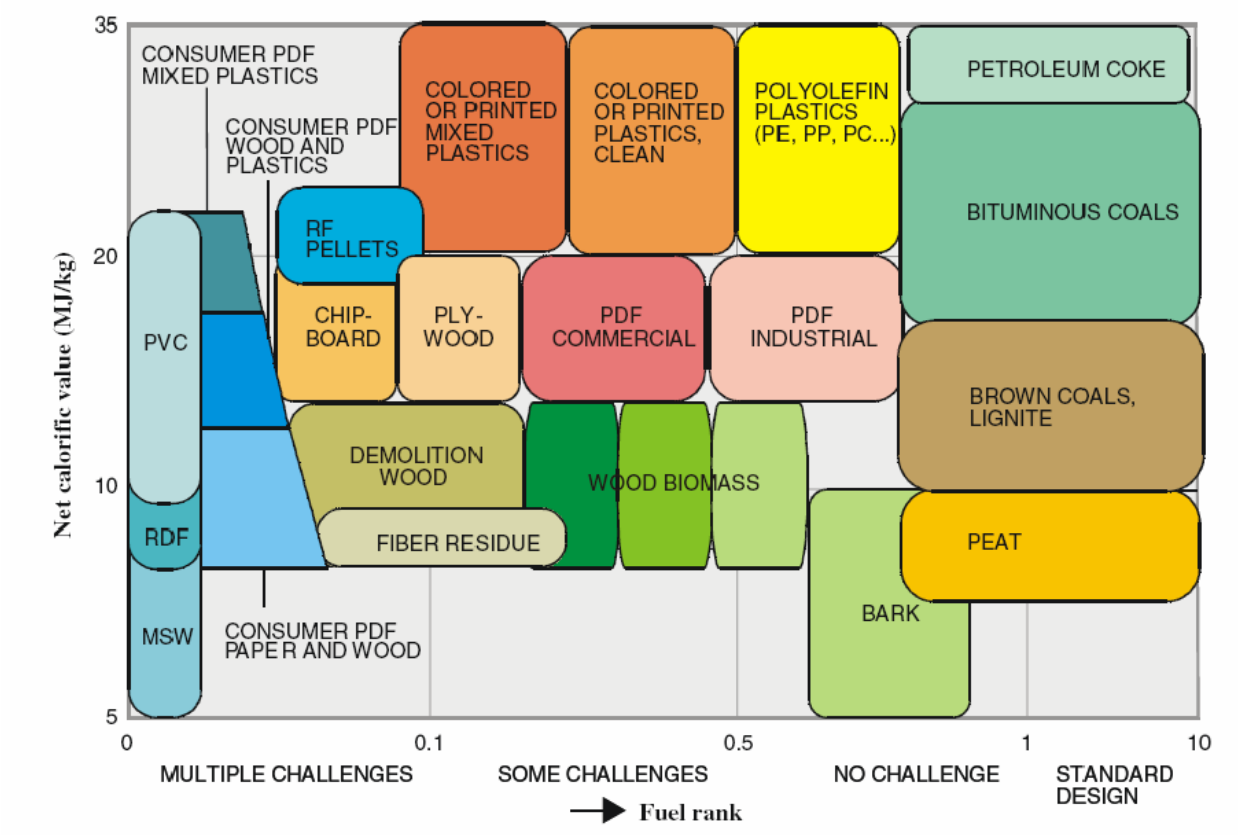

Figure 1-1.1 Different variety of fuel used in FBC[17]

When determining the classification of fluidized beds, the regimes that are utilised in the beds are taken into consideration. The type of regime that will be applied is going to be decided by how quickly the gas rate is increased that is being delivered to the bed. Figure 1.2 provides a summary of the many different fluidized bed regimes that can be put into practise. This category contains a variety of different regimes, including fixed bed, bubbling bed, slugging bed, turbulent bed, rapid bed, and pneumatic bed, among others. Whenever the gas velocity in the fixed bed is relatively

low, the drag force that acts to lift the bed is maintained at a level that is relatively low. This keeps the bed from sinking. When the solids begin to migrate upward as a result of an increase in the velocity of the gas in the system, this results in the formation of a fluidized bed. There are many distinct fluidization regimes that can be observed, and each of these can be linked to the various speeds at which the gases are moving. In recent years, the bubbling fluidized bed boiler and the circulating fluidized bed boiler have been the two types of fluidized bed boilers that have seen the greatest amount of use for the purpose of producing energy. Both of these boilers are fluidized beds. The fluidized beds that contain gas or liquid are heated in both of these boilers, which serve the same purpose. When air is injected into the bubbling fluidized bed that is located at the bottom of the distributor, it causes the formation of bubbles in the solid phase of the emulsion, which then rise to the surface. This occurs because the air triggers the formation of bubbles in the solid phase of the emulsion. As the bubbles rise, they encounter one another. Because of this, larger bubbles are produced when the smaller bubbles combine. At some point, the bubbles that were formed will burst on the surface of the water where they were formed. This will happen at some point in the future. This is the method that is utilised in order to combine the solids into a single homogenous entity. The air that is supplied from below is subject to regulation so that the bed can remain in the bubbling regime and so that there is minimal solid migration. This is done in order to keep the bed in the bubbling regime. It is necessary to do this in order to maintain the bubbling state of the bed. When it comes to the circulating fluidized bed, the air that is supplied is done so in such a way that the solids migrate in such massive quantities that it is impossible to count them all. In other words, the air is delivered in a manner that enables this to occur. The cyclone will recycle the solids it catches from the bed so they can be used as bedding once again. This procedure will continue until all solid waste has been collected.

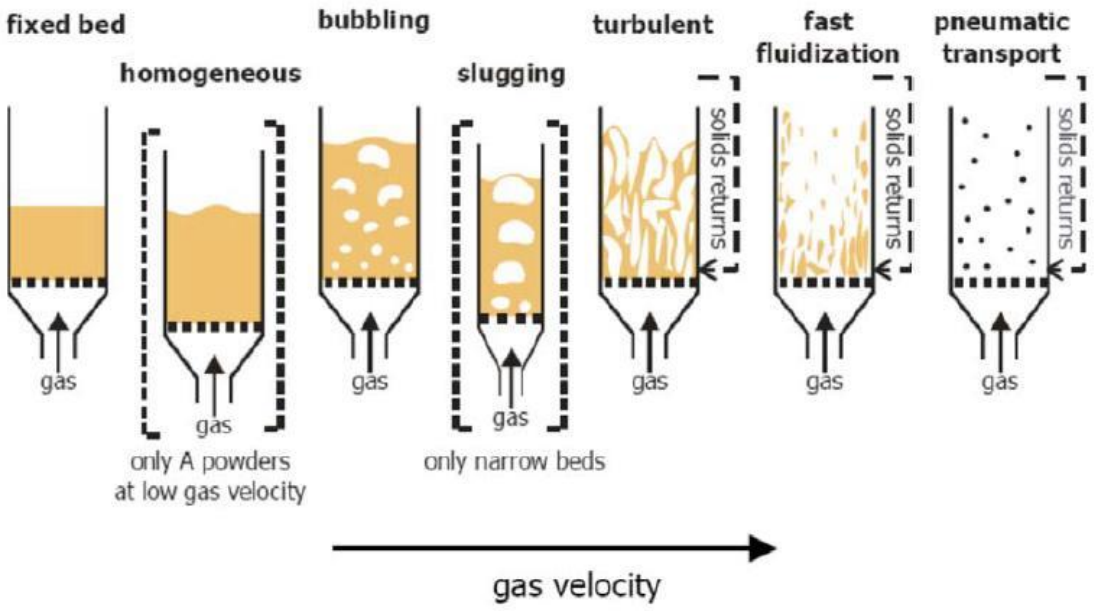

Figure 1-2.Flow Regimes of Fluidized Bed [18]

The following are some categories that can be used to describe the advantages that fluidized bed boilers bring to the table:

1- Since the fuel particles behave in a manner that is analogous to that of liquids, the system can be easily controlled, and the user needs to exert very little effort in order to do so.

2- The elimination of hot spots and the establishment of an even temperature distribution across the entire area will both be the direct result of ensuring that the solids are thoroughly mixed. The procedure can be carried out in a dependable and uncomplicated manner provided that this step is followed.

3- In large reactors, materials can be pumped between two fluidized beds in order to facilitate the transfer of heat between the beds. This helps the reactor operate more efficiently. The work is carried out in enormous reactors.

4- Heat and mass transfer coefficients that are significantly higher than the average for the material. As a direct consequence of this fact, heat exchangers are required to have a total surface area that is a great deal less than what it was in the past.

5- Fluidized bed boilers offer greater versatility in terms of the types of fuels that can be burned in the boiler. This allows the boiler to be used for a wider range of applications. Because of this, it might work with fuels that have a low calorific value and a high percentage of moisture in them. In other words, it depends on the specifics of the fuel.

6- As a result of the lower temperatures that are required for operation, the FBC emits a significantly lower level of 6-NO_x than a conventional combustor does. This is due to the fact that the FBC operates at a lower temperature (800~900℃).

7- During the process of combustion that takes place in the furnace, it is possible for some of the SO2 that is present in the FBC to be absorbed. because it allows the substance to be absorbed in a fluidized bed while maintaining a low combustion temperature and making use of a limestone system. This is made possible by the fact that it is a multi-step process.

8- Fluidized bed combustion (FBC) systems provide higher combustion efficiencies when compared to systems that burn powdered coal.

9- The process of removing ash from FBCs has been streamlined to make the procedure less complicated and more user-friendly.

The following is a list of some of the drawbacks that are associated with the use of fluidized bed boilers:

1- The presence of fine particles makes it difficult and inefficient to estimate the flow of gas in bubble beds, which in turn makes measuring gas flow difficult. This is because measuring gas flow is difficult.

2- The rapid mixing of particles in the substrate, which is the primary source of the issue, is what leads to the heterogeneous shelf life that develops in the reactor. This is the root cause of the problem.

3- The surfaces of pipelines and ships may become worn and damaged as a result of the collision of particles with those objects.

4- It will need to be replaced after the particles have been pulverised and transported using gas. The transportation of the particles will be done using gas. This particular line of inquiry has its

primary point of interest focused on the bubble fluidized bed as its central topic of investigation.

1.4 Fluidization

The term "fluidization" refers to the transformation of solid particles into a condition similar to that of a fluid while they are suspended in a gas or liquid. Fluidized beds have found widespread application in a variety of industrial processes, including those involving the gasification, pyrolysis, and combustion of a wide range of particulate materials, including biomass. The benefits of fluidization include high heat transmission, temperature regulation and uniformity, favourable gas-solid contact, and the ability to work with a diverse set of particle characteristics. Figure 1.3 shows the fluidization.

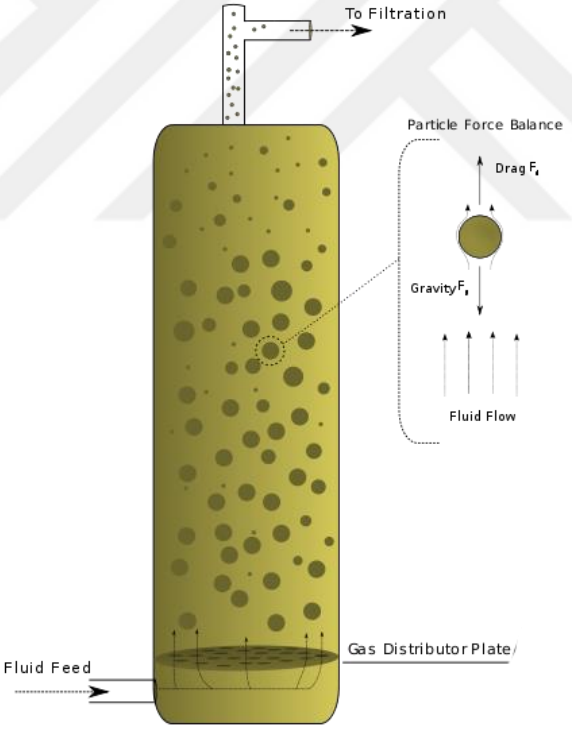

Figure 1-3. Descrption of fluidization

Fluidized bed

A fluidized bed is a term that refers to a column that is made up of a collection of solid particles and that is supported by a plate that is perforated. The fluid will have passed through the supporting plate, the particle bed, and the fluid by the time it reaches the top of the column. Even though the particles are subjected to the drag force of the fluid flow at low flow rates, their weight is what keeps them in place. Particles will become suspended in the flow at a specific velocity, and the force of drag will counteract the weight of the particles. Because of the striking resemblance between this suspension's behavior and that of a viscous liquid, the terms fluidized particles and fluidization were coined to describe it. We are primarily interested in the use of fluid beds for gasification, which is one of the few technologies to take advantage of the tendency of solid particles to behave similarly to liquids.

An increase in the fluid flow rate beyond what is necessary for the suspension to become fluidized in the beginning will result in the suspension becoming more expansive. The formation of bubbles is referred to as bubbling, aggregative, or heterogeneous fluidization, while uniform expansion is referred to as homogeneous or particulate fluidization. Both of these terms refer to fluidization. The bubbles are reasonably stable formations because they rise through the bed, have strong borders, and are almost entirely devoid of particles. When the volume of fluid passing through the column increases, the bubbles expand, and if the column is sufficiently thin, the bubbles can eventually fill the cross-section and become slugs. Even further increases have the potential to bring about a collapse in the bubbling, which would ultimately result in the bed being moved out of the column.

Because of the bed's ability to expand and reduce flow resistance, the pressure drop does not significantly increase after the incipient fluidization stage, even though the fluid flow velocity is increased. Due to the fact that the entrained particles present a lower flow resistance, the pressure drop will eventually decrease when entrainment occurs in the system.

Minimum fluidization:

In order to determine the minimum fluidization velocity, the pressure drop method was applied in both the experiments and the process of modelling. This was done so that the results could be compared. The pressure drops across the entirety of the fluidized bed, represented by the symbol P, is measured at a variety of different superficial gas velocities. This allows for more accurate

results. When utilising this approach, the velocity of the gas is first increased and then decreased over the course of the process. It is necessary to take this step-in order to prevent the hysteresis that is typically observed as a direct result of utilising this method. The minimum fluidization velocity can then be calculated based on the data for the decreasing superficial gas velocity. This can be accomplished by first plotting two lines that roughly represent the pressure drop under fixed bed conditions and then fluidized bed conditions, and then locating the point at which these two lines intersect with one another.

When trying to determine an accurate minimum fluidization velocity all the way through the model, it is absolutely necessary to have a thorough comprehension of the function that the close pack factor plays in the process. The amount of pressure loss that takes place in the region characterised by the fixed bed is influenced by the value of the close pack factor. This is because the pressure loss in the region of the fluidized bed is only dependent on the weight of the suspended particle bed. This is the reason why this is the case. The pressure drop in the fixed bed will increase as the close pack factor increases. This will cause the slope of the fixed bed line to become steeper as the close pack factor increases. This, in turn, will cause the intersection of the fixed and fluidized bed lines to shift to lower superficial gas velocities. This will occur because the superficial gas velocities will be lower. As a direct consequence of this fact, the minimum fluidization velocity that has been predicted will decrease in proportion to the increase in the close packing factor.

The rate of air flow had to be gradually slowed down until the particles were able to settle in order to determine the minimum fluidization velocity. This was done so that the minimum fluidization velocity could be determined. It was determined that the minimum fluidization velocity for our simulation should be the velocity at which the air was flowing at this point. In order to calculate the Reynold's number and the minimum fluidization velocity, respectively, we made use of two distinct formulas, one to find the Reynold's number, and the other to find the minimum fluidization velocity. Specifically, we used one formula to find the Reynold's number, and the other formula to find the minimum fluidization velocity.

The minimum fluidization Velocity Calculations:

The pressure drop that occurs when air moves over a packed bed is approximately proportional to the superficial velocity of the air. In order to transition from a solid state to a fluidized one, the velocity of the gas is continuously increased. When a bed is allowed to stand on its own, it will reach a point that is referred to as the minimum or incipient fluidization point. This is the point at which the mass of the bed is directly suspended by the flow of the air stream. The velocity of the fluid in question is referred to as the "minimum fluidization velocity," or simply "minimum velocity".

$$\frac{\rho_g D_{sv}^3(\rho_p - \rho_g)g}{\mu^2} = \frac{150(1-\varepsilon_{mf})\rho_g D_{sv}}{\varepsilon_{mf}^3 \mu} U_{mf} + \frac{\rho_g^2 D_{sv}^2}{\varepsilon_{mf}^3 \mu^2} U_{mf}^2 \quad (1)$$

$$Dv = 1.13\, Dp \quad (2)$$

$$Dsv = 0.87\, Dp \quad (3)$$

$$\psi = Dsv/Dv \quad (4)$$

$$€ = \frac{Voidage\ Volume}{Volume\ of\ particles + voids} \quad (5)$$

Sieve size D_P is the minimal square aperture through which the particle can travel. Volume diameter D_V is the radius of a sphere with the same volume as the particle in Eq.2. Surface Volume diameter D_{SV} in Eq.3 is the diameter of a sphere having the same external surface area /volume as the particle. Sphericity (Ψ) is defined as the surface area of an equivalent volume sphere divided by the particle's surface area. A mass of material has particles that rest on top of one other due to gravity to form a packed bed. However, depending on the particle shape and packing properties, a certain volume of space in between the particles remains vacant; this area is referred to as voidage(€). Minimum fluidization velocity (U_{mf}) is minimum velocity of complete fluidization is the minimal velocity necessary to fully sustain the solids.

1.4.1 Hydrodynamics of Fluidized bed:

It is not possible to fluidize different kinds of particles in an effective manner even if it were possible. Particle size is a crucial variable in fluidization. It is possible to categorise the particles according to both their density as a whole and the size of the particles that make up the whole. When working with particles that are classified as Category (C) and have a diameter of less than 30 microns, fluidization can be an extremely challenging process to accomplish. Again, the challenge lies in fluidizing particles that belong to Category (A), have a size range that falls between 20 and 100 microns, and demonstrate significant expansion when the required minimum fluidized gas velocity is exceeded. When it comes to fluidization, the best particles to work with are those that are classified as belonging to Category (B) and have a size range that falls between 400 and 500 microns. As a result, the classification was related to the influence of the average particle size and particle density on the properties of the fluidized layer, as depicted in Figure 1.4.

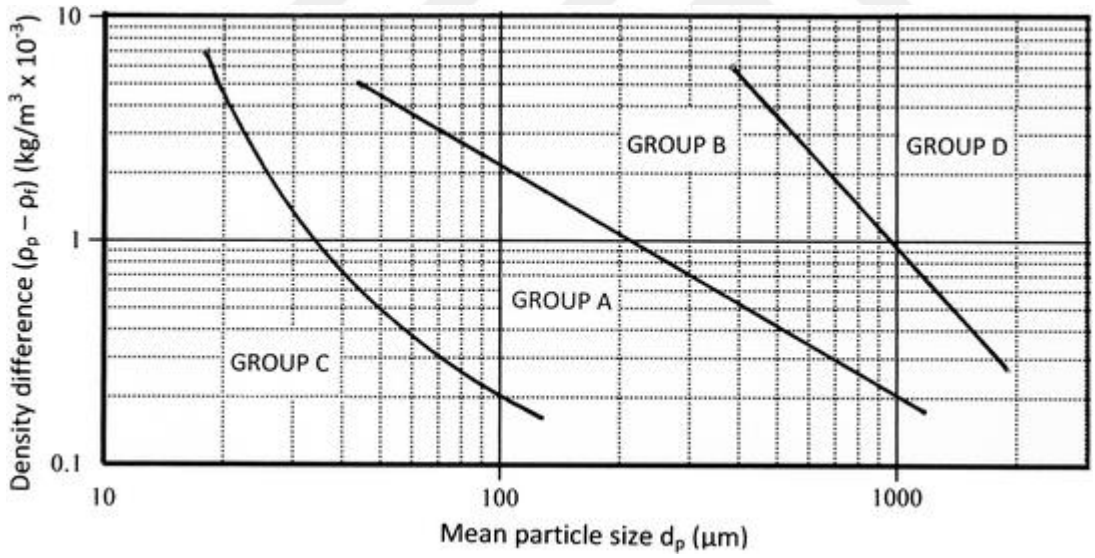

Figure 1-4 Diagram of the Geldart classification of particles[19]

1.4.2 Bubbling Fluidized Bed (BFB) Boilers

The bubbling motion is a characteristic of one variety of fluidized bed that is more common than

any other. There are approximately 10,000 BFB boilers thought to be operational around the world at the present time. In addition to a furnace, the BFB boiler includes a section that is dedicated to the convective exchange of heat. These are the two components that, when put together, constitute the boiler. The heating device is made up of two distinct parts that are easily detachable from one another and can be put to separate uses. It is made up of freeboard parts that are situated above the bubbling bed of combustible solids as well as the bed itself. In addition to this, it also includes the bed itself. In addition to that, the bed itself is included in the package. In terms of its operational characteristics, the convection section performs its duties in a manner that is comparable to that of a conventional boiler. The pressure settings of a BFB boiler furnace can be adjusted to either atmospheric or enhanced levels, depending on the requirements of the user. These processes can either use a pressurised fluidized bed combustion (PFBC) setup or an atmospheric fluidized bed combustion (AFBC) setup [20]. Both of these setups are referred to as fluidized bed combustion . The use of a bubbling fluidization regime is where bubbling fluidization boilers, also known as BFB boilers, get their name from. This is suggested by the name of these types of boilers. The fluidizing air that is supplied by the BFB boilers ought to make it possible to fluidize the solids that are present in the bed. According to the findings of some studies, the minimum fluidization velocity can be up to three or four times lower than the maximum fluidization velocity. The information was obtained by comparing the two velocities. In a BFBC, fuels such as coal and petroleum coke are pulverized into fragments ranging in size from 0 to 10 millimetres in one or both directions. The size of the crushed fuels generated is mostly governed by a combination of factors, such as the rank of the coal and the type of fuel supply being utilized. The external air that is brought into the system serves two unique purposes: it oxidizes the system's components and works as a fluidizer. The air is responsible for both functions when it's in motion. Following this step, the gases that are produced by the exhaust flue are utilised to pre-heat the pressurised air, and this air is then distributed throughout the bed. The velocity of the fluidizing air as it is typically introduced into the reactor ranges anywhere from 1.2 to 3.7 metres per second, depending on the normal rate at which it is introduced. Because the maximum amount of fuel that can be burned is determined by the amount of fuel that can be burned, the rate at which air is forced through the bed is an important factor in determining the maximum amount of fuel that can be burned, as this maximum amount is determined by the maximum amount of fuel that can be burned. The majority of bubbling fluidized bed boilers have evaporator tubes constructed directly into the bed of sand,

fuel, and limestone that is being heated. This is the case with almost all of these boilers. The temperature of the bed can be kept at a stable level by removing excess heat using these tubes, which were designed specifically for that purpose. The depth of the bed is typically measured to be somewhere in the range of 0.9 to 1.5 metres in length on average. The depths typically fall within this range. With each millimetre of increased bed depth, the pressure will decrease by precisely 25,4 millimetres of water. As a result, a far smaller proportion of the material in the bubbling fluidized bed is discarded. This is a direct consequence of the events that have transpired. For every tonne of fuel that is consumed, only two to four kg of solid waste may be recycled. This ratio cannot be sustained. Figure 1.5 illustrates a BFB combustor.

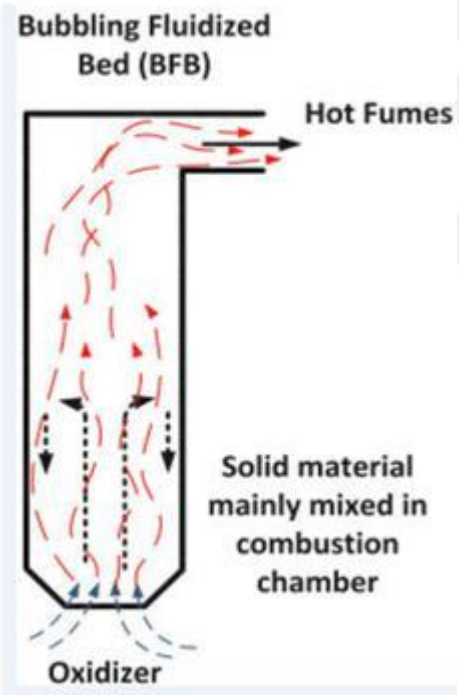

Figure 1-5 Bubbling Fluidized Bed Boiler[21]

1.4.3 Circulating Fluidized Bed (CFB) Reactors

One of the reasons there is so much interest in the technique of circulating fluidized beds is that it allows for a low-temperature, fuel-flexible burning process. This is one of the reasons why this technology has gained so much interest. The circulating fluidized bed reactor is one of the types of reactors that is used for the transformation of solid fuel more frequently than any other type.

This is because it is one of the types of reactors that can produce the highest level of energy efficiency. The CFB technology has the potential to generate power in a manner that is both beneficial to the environment and cost-effective if it makes use of a wide variety of carbon-free fuels, such as biomass and recycled waste, in addition to carbon-containing fuels, such as petroleum and coke. In this scenario, the CFB technology could generate power in a manner that is both environmentally friendly and cost-effective. Fuels that have no impact on the environment in terms of carbon emissions include, among other things, biomass and recycled waste. Because it can burn a wider variety of fuels than any other kind of reactor, it has a significant advantage over the constraints that are imposed by conventional combustion, which is a significant advantage. Before the conventional procedures of coal combustion systems can be utilised, the fuel must first be dried, and then it must be finely grinded. Both of these steps are necessary before the coal can be burned. After carrying out each one of these procedures to its conclusion, the fuel can at long last be introduced into the oven. Following the cutting of the fuel into large chunks, it is then deposited into fuel chutes that are connected to ports in the lower section of the CFB's furnace. Because of this, the steps that came before are no longer necessary. Traditional boilers, on the other hand, burn the fuel in a massive flame that is brought to an extremely high temperature. This creates the necessary heat for the boiler. These procedures are in no way, shape, or form mandated by the CFB in any capacity. CFB technology makes use of a flameless combustion process that involves the utilisation of circulating hot solids in order to burn fuel in a manner that is both effective and kind to the environment. This allows the technology to burn fuel in a more environmentally friendly manner. This enables the technology to burn fuel in a manner that is friendlier to the environment than previous methods. Its low and consistent combustion temperature prevents the formation of nitrogen oxides and makes it possible to inject limestone, which absorbs acid gases as the fuel is burned. Both of these benefits are a direct result of the low and consistent temperature of its combustion. Both of these advantages are a direct consequence of the low and stable temperature at which its combustion takes place. These two factors help bring about a decrease in the overall levels of air pollution. Because the ash that is produced from the fuel does not melt during the combustion process, the CFB is the type of furnace that generates the least amount of emission overall. This is due to the fact that the CFB is the most efficient type of furnace. The hot solids are able to effectively transmit their heat throughout the entirety of the boiler as a result of the clean heat transfer surfaces, which simultaneously lowers the risk of fouling

and corrosion. This allows for the effective transmission of heat from the hot solids. The amount of pollution that plants cause has decreased as a direct result of this, which has led to an improvement in the environment. It is possible to achieve a very high level of plant reliability with only very minor amounts of maintenance being required in order to support the accomplishment of a very high level of combustion efficiency. This will allow the plant to support the achievement of the very high level of combustion efficiency. The collection of the solid particles that are generated by the furnace is the responsibility of solid separators, which are cooled by steam. The vast majority of the solid particles that were previously present in the furnace are subsequently reintroduced into the furnace after being collected by the steam-cooled solid separators and then returning there after being cooled by steam. On board the Trek, the particles pass through a section of the heat exchanger that has a particularly high-performance rating prior to being recirculated into the furnace. This is the part of the plant where steam coils are submerged in a bubbling bed of hot solids in order to efficiently generate high temperatures and superheat steam. This ultimately leads to a further reduction in the plant's operating costs as well as its emissions.

In CFB reactors, the reactor is loaded with a mixture of solid fuel and sand or ash, which is then heated to a high temperature. This process is repeated until the desired temperature is reached. This procedure is carried out several times until the required temperature is achieved. After that, it is time to let the mixture warm up the reactor so that it can continue operating. In the initial stage of this process, which consists of bringing the solid particles to the top of the reactor, air is the agent that is responsible (or steam or oxygen). When applied to industrial settings, the particle terminal velocity is typically much slower than the gas superficial velocity, which is typically between 4 and 6 metres per second. This is because the particle terminal velocity is measured at the particle's final resting place. This is due to the fact that the terminal velocity of a particle is measured at the point where the particle comes to a complete stop. The average diameter of the material particles grows to somewhere between 0.05 and 1 millimetre when they are subjected to repeated passage through the system. Very high levels of solid mixing are produced as a result of the turbulent regime that the gas and solid mixture encounters in CFB reactors. Because of this, the superficial gas velocities that these reactors produce are noticeably higher than the average value. In addition, the heat transfer coefficients are extraordinarily high, ranging from 100 to 200 W/m2 °C depending on the situation.

CFB reactors are constructed out of a riser, which is the primary location for the majority of the

reactions, a cyclone, which separates the solid from the hot gas, a downcomer, which enables solids to be introduced into the reactor, and a non-mechanical solid circulation valve, which enables solid particles to be recirculated back into the reactor while preventing reverse gas flow. In the vast majority of situations, loop seals and L valves are utilised to provide assistance in the process of solids being circulated through a system. This is the case because these components help prevent leaks and ensure proper flow. Loop seals are a type of non-mechanical valve that are typically utilised in applications that are carried out on an industrial scale. The fluidized bubble bed, which functions as a pressure barrier between the reactor and the downcomer, is the element of a loop seal that is considered to be the most fundamental. This bed will serve as the basis for the construction of the loop seal. In addition to that, it is the duty of this bed to reintroduce any solid particles that had been removed from the reactor at an earlier time.

2 METHODOLOGY

2.1 Numerical Method

When it comes to obtaining CFD solutions, there are many different options available, and the right one must be chosen depending on the flow type (incompressible, compressible, turbulent, laminar, etc.). First and foremost, Barracuda offers a variety of equation solvers, including pressure-based equation solvers and density-based equation solvers respectively. For the purpose of CFD analysis, a pressure-based solver was chosen as the equation solver because it offered superior convergence performance with only a negligible loss in accuracy. Numerical simulations were carried out utilizing the Barracuda software's CPFD approach. The CPFD method is used to solve the three-dimensional particle and fluid governing equations [22]. The gas-solid phase drag forces, which account for the gas-particle and particle-particle interactions in addition to the pressure gradient and gravity, are used to estimate the particle acceleration. In the CPFD approach, the appropriate conservation equations for gas flow are stated as [23];

$$\frac{\partial(\theta_f \rho_f)}{\partial t} + \nabla\left(\theta_f \rho_f u_f\right) = 0 \tag{6}$$

$$\frac{\left(\theta_f \rho_f u_f\right)}{\partial t} + \nabla\left(\theta_f \rho_f u_f u_f\right) = -\theta_f \nabla p \; + \; F \; + \; \theta_f \rho_f g \; + \; \nabla(\theta_f \tau_f) \tag{7}$$

θ_f stands for the volume fraction, u_f for the gas velocity, p for pressure, F represents the body force and τ_f is the viscous stress. The viscous stress is given by;

$$\tau_{f,ij} \; = \; \mu_f \left(\frac{\partial ui}{\partial xi} + \frac{\partial uj}{\partial xi}\right) - \frac{2}{3}\, \mu \delta_{ij}\, \frac{\partial uk}{\partial xk} \tag{8}$$

The acceleration of particle is obtained by [24]:

$$\frac{du_p}{dt} = D_p\,(u_f - u_p) - \frac{1}{\rho_p}\nabla p - \frac{1}{\rho_p \theta_p}\nabla \tau_p g \qquad (9)$$

where u_p and θ_p are the velocity and the volume fraction of the particles respectively. D_p and τ_p are, the drag function and the stress tensor. Eq. 10 expresses the calculation of particle volume fraction as:

$$\theta_p = \iiint f V_p dV_p d\rho_p du_p \qquad (10)$$

where, V_p is volume of the particle. Moreover, in CPFD, the particle normal stress (τ_p) is used to calculate particle-to-particle collision which takes the adjacent particles contribution on a particle momentum into account.

The τ_p is given by [25] :

$$\tau_p = \frac{P_s {\theta_p}^{\beta}}{max[(\theta_{cp} - \theta_p), \varepsilon(1 - \theta p)]} \qquad (11)$$

where θ_{cp} represents the close pack volume fraction. The static pressure is P_s and β stands for Interphase momentum transfer coefficient and ε is Volume fraction.

2.2 Turbulence Model

Nearly every fluid flow that we come across in daily life is turbulent. The flow in and around cars, airplanes, and buildings are common examples. Turbulent boundary layers surround and follow solid bodies, such as cars, airplanes, and buildings. Additionally, the flow and combustion in engines—in both gas turbines and combustors as well as piston engines—are quite turbulent. Therefore, it is likely that the fluid flow we compute will be turbulent. In order to account for flow turbulence in our calculations, Baracuda software uses Large Eddy Simulation (LES) approach [26]. Large Eddy Simulation (LES) approach represents the most promising future methodology for modelling the unsteady and intermittent behaviour of large-scale turbulent eddies present in

many industrial flows involving both complex physics and complex geometry[27]. The filtered Navier-Stokes equations for the gas phase, as well as the filtered transport equations for energy and species mass conservation, are solved in LES[28].

2.3 Drag Models

The choice of drag model used in CPFD modelling of gas-solids flow has a substantial impact on the outcomes of the simulation. As a result, it is essential to conduct experiments using a variety of different drag models in order to ensure that the outcome is independent of the drag model. The simulation was analysed using not one, but two distinct drag models: Wen Yu-Ergun and EMMS. This was done to demonstrate that the results were independent of the drag models. As a result of the model having a constant mass flow rate at both its inlet and its outlet, a steady state solution was accomplished. This indicates that the solution was time independent. The following is an explanation of how particles are affected by drag force:

$$F_P = m_p D(u_g - u_p) \tag{12}$$

where m_p and D represent the particle mass and the drag function, respectively. In most of the models, the drag function depends on flow conditions, geometry and the drag coefficient Cd.

2.3.1.1 Wen-Yu/Ergun Drag Model:

The drag model, which represents the interaction between the gas and particle phases, is crucial to the success of the simulation. The drag model utilized here is a blend of Ergun's [29] and Wen and Yu's research [30]. Wen and Yu investigated systems with solids volume fractions between 0.01 and 0.61, whereas the Ergun correlation was created for systems with particle volume fractions between 0.47 and 0.70. In the drag model of the Wen-Yu model mixed with the Ergun model, the Wen-Yu correlation is used for solid volume fractions less than 0.75 $\boldsymbol{P}_{\mathrm{CP}}$. In comparison, the Ergun equation is utilized for solid volume fractions more than 0.85 $\boldsymbol{P}_{\mathrm{CP}}$, where $\boldsymbol{P}_{\mathrm{CP}}$ is the solid volume fraction at close packing. For the solid volume fractions between 0.75 $\boldsymbol{P}_{\mathrm{CP}}$ and 0.85 $\boldsymbol{P}_{\mathrm{CP}}$, a transition function is employed to prevent potential numerical simulation issues caused by the discontinuity and abrupt transition in the drag model. In this investigation, the particle-phase

volume fraction at close packing is 0.64; hence the solid volume fraction range between 0.48 and 0.54 marks the transition between the two correlations. The drag model of Wen-Yu correlation mixed with Ergun correlation is displayed below. D is the force of drag, D_1 is the force of drag according to the Wen and Yu model, D_2 is the force of drag according to the Ergun model, C_d is the drag coefficient, and R_e is the Reynolds number.

The Wen-Yu/Ergun model is defined as:

$$C_d = \begin{cases} D_1 & \theta_p < 0.75\theta_{cp} \\ (D_2 - D_1)\dfrac{\theta_p - 0.75\theta_{cp}}{0.85\theta_{cp} - 0.75\theta_{cp}} & 0.75\theta_{cp} \le \theta_p \le 0.85\theta_{cp} \\ D_2 & \theta_p > 0.85\theta_{cp} \end{cases} \quad (13)$$

2.3.1.2 EMMS Drag Model:

The energy minimization multiscale model, sometimes known as EMMS, is a heterogeneous drag model commonly used to simulate gas–solid fluidized beds[31].

$$f_e = \begin{cases} \dfrac{1}{180\theta_P}\left(150\dfrac{\theta_p}{\theta_g} - 1.75Re\right) & \theta_g < 0.74 \\ (1 + 0.15Re^{0.678})\omega & \theta_g \ge 0.74 \text{ and } Re < 1000 \\ 0.44\dfrac{Re}{24}\omega & \theta_g \ge 0.74 \text{ and } Re \ge 1000 \end{cases} \quad (14)$$

$$\omega = \begin{cases} -0.5760 + \dfrac{0.0214}{4(\theta_g - 0.7463)^2 + 0.0044} & 0.74 < \theta_g \leq 0.82 \\ -0.0101 + \dfrac{0.0214}{4(\theta_g - 0.7789)^2 + 0.0040} & 0.82 < \theta_g \leq 0.97b \\ -31.8295 + 32.895\theta_g & 0.97 < \theta_g \leq 1 \end{cases} \quad (15)$$

2.4 Experimental Setup

The referral CFD model needs to be validated using the experimental data before the refinement studies of the riser design can begin. This will allow the researchers to determine whether or not the reliability level of the model is appropriate. Because the primary objective of employing a CFD model is to make improvements with respect to the reference ejector design, and because making these changes needs to be done using a verified model, the CFD model must be validated. The reference riser model is constructed out of a plexiglass material that is transparent. After the mass flow controller (mfc) was used to measure the flow rate of the compressed air, the air was then fed to the riser. The level of ambient temperature was determined using a thermocouple and was assumed to be the temperature of the feeding air.

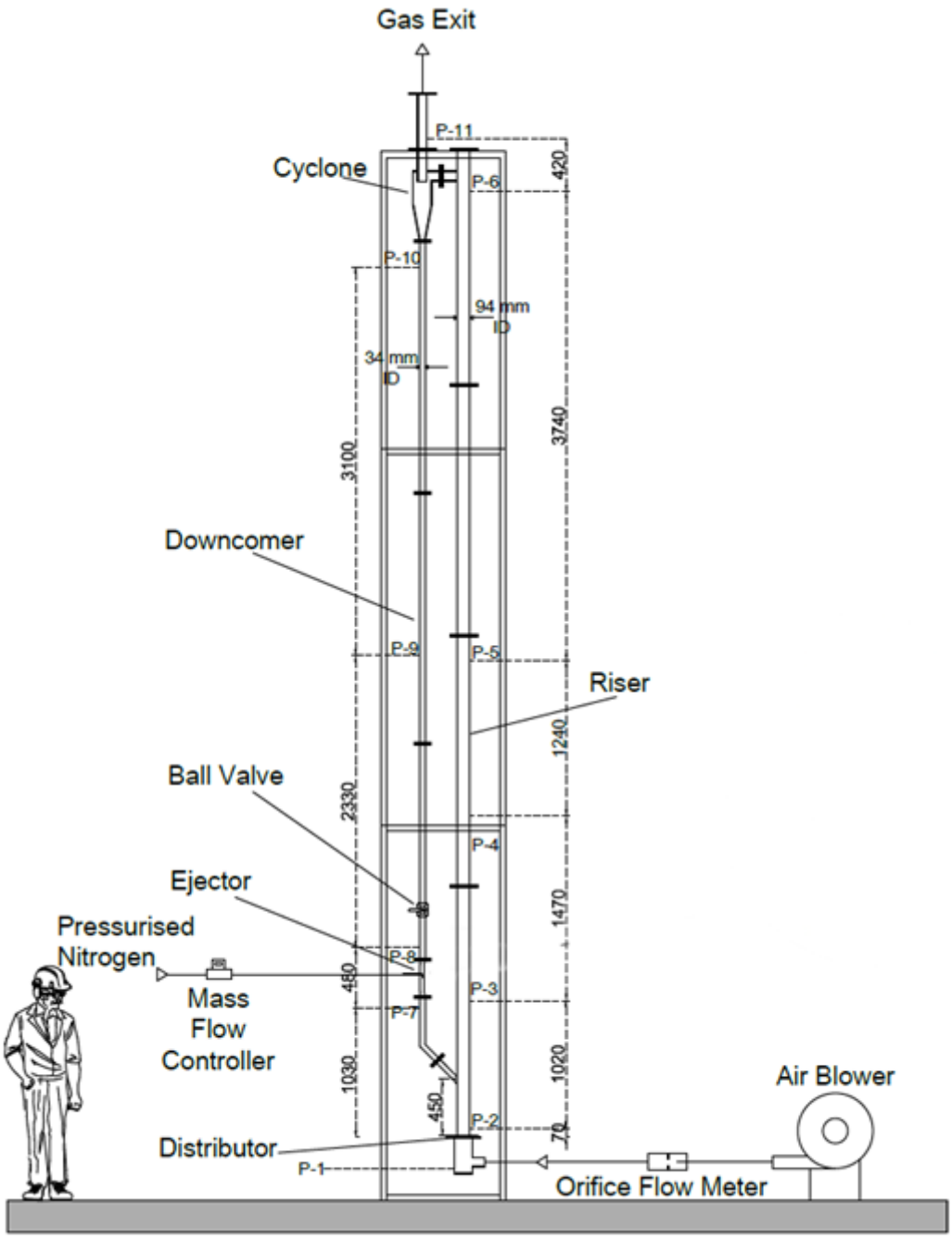

Figure 2-1 Experimental CFB Cold Model [32]

Fig.2.5 depicts the assembly of the cold model CFB system. System components include a CFB riser, cyclone separator, ejector at the downcomer, and return conduit to the riser. The riser's height is 7800 millimetres. The riser has an inside diameter of 94 mm and the downcomer has an inside

diameter of 34 mm. The downcomer features an ejector with a tube measuring 25.7 mm in width and a nozzle measuring 2 mm in width. 140 mm is the inner diameter of a cyclone separator. The ejector is mounted on the downcomer, which connects the riser and the cyclone. The downcomer is attached to the riser at an angle of 450 degrees. Just above the dense bed, the recycled solid material is added to the riser. The air blower that supplied the fluidization air was controlled by the frequency controller (rpm control of blower motor). The orifice flow meter was used to measure the velocity of the fluidization air, while the blower motor's revolutions per minute were used to adjust the flow rate. Fluidization air traveled from the windbox and the distributor plate to the riser. The distributor plate is made of fabric and is supported by steel mesh. Eleven pressure ports along the solids circulating loop could be used to determine the pressure profile of the system. There was one pressure port on the windbox, five on the riser, four on the downcomer, and four at the end of the cyclone. A data logger was utilized to record the pressure at each port over a period of time. During the cold tests, the solid circulation rate is measured at the downcomer using a ball valve. Pressurized nitrogen served as the ejector's driving gas. The flow rate was altered by a mass flow controller (MFC), which combines a control valve and flowmeter.

2.5 Numerical Model:

Barracuda Virtual Reactor® v17.4.0, a computational fluid dynamics (CFD) tool, was utilised in this project so that the outcomes of the real riser could be simulated. This allowed for a more accurate representation of the riser's performance. The Barracuda Virtual Reactor® is a simulation tool that provides particle-fluid dynamics, and it is used for the purpose of designing, troubleshooting, and optimising industrial fluidized systems. Two distinct steps make up the primary process that CFD software employs in order to solve problems. This process can be broken down into these two steps. In the first stage of the process, the physical model is discretized into finite volumes (elements) in order to generate a set of algebraic equations and make it possible to apply partial differential equations as a finite volume approach. This is done so that the model can be analysed using a finite volume approach. The use of the finite volume approach is now feasible as a result of this. In the second stage of the CFD method, you will be tasked with solving a system of algebraic equations in order to find an approximation of a solution to the aforementioned system.

In order to accomplish this goal, it would have been necessary to set a few different variations. The mesh type, air quality, bed materials, particles specification, initial and boundary conditions, solver, and hydrodynamic calculations were some of the various factors that were taken into consideration.

2.5.1 CFD model structure

In this part CFD model structure is explained with detail.

2.5.1.1 distributer plate:

Because of the distributor plate's extremely minute pores, it is not possible for fine particles to enter the wind box. This distributor plate features 715 holes that are 1 mm in diameter each. The holes are angled at a 45-degree angle so that there is as little backflow of solid material as possible. With a superficial gas velocity of 6 m/s through a riser, gas velocities through the holes are 40 m/s.

2.5.1.2 Riser:

In the course of the hot test facility, it was decided that the riser's dimensions should be the same as those of the hot test facility. The riser is 94 millimetres in diameter and 7800 millimetres in height. Figure 2.2 depicts the riser's overall layout and construction. The degree to which the wall of the riser is smooth affects the nature of the interaction between the particles and the wall. In order to accurately simulate the interaction between particles and walls, the normal to wall momentum retention parameter was set to 0.5, and the tangent to wall momentum parameter was set to 0.85.

Figure 2-2 CFB riser of Cold CFB model

2.5.2 Global Setting

A set of global settings was used to simulate the cycle. Earth's gravity was set at 9.807m/s^2 during simulation. Set the temperature to 300˚ K for the isothermal flow.

2.5.3 Base Materials

2.5.3.1 Air:

For preliminary analysis, air is selected as the working fluid. Fluid density is not constant because the flow is compressible, as it is determined by ideal gas relations.

2.5.3.2 Bed material(silica):

Bed material was silica sand, whose weighted arithmetic mean diameter was 644 microns according to sieve analysis. Densities of the bulk and particles were 1450 kg/m3 and 2545 kg/m3, respectively.

Table 2.1 Bed material specifications

Bed material (silica sand) bulk density	1450 kg/m3
Bed material (silica sand) particles density	2545 kg/m3
Close pack volume fraction	0.65
maximum momentum redirection from collision	40%

2.5.4 Particles size distribution:

In the real model, the size distribution is indicated in only 3 points, for which we added 2 points to the diagram by interpolation to make the distribution more uniform. The bed material was silica sand, its size distribution can be seen in Figure 2.3. According to the Geldart powder classification criteria, the sand particles used in CFB cold tests corresponded to Group B particles [33]. The sand's sphericity was 0.9.

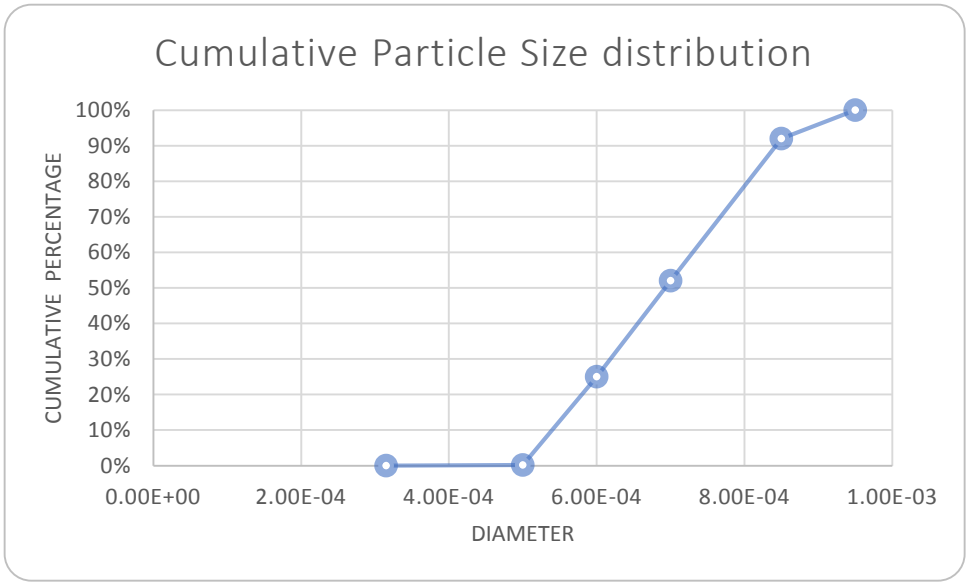

Figure 2-3 Cumulative particle size distribution

2.5.5 Initial Conditions

2.5.5.1 Fluid initial conditions

It was assumed that conditions of standard pressure and temperature existed. As a direct consequence of this, the temperature was set to 300 Kelvin, and the pressure was set to 101325 pascals. Because there was no motion in the air, the velocity was also set to 0 metres per second.

2.5.5.2 Particles initial conditions:

As in the experiments, the amount of silica sand in the riser was assumed to be 3kilograms, which corresponds to 29.8 cm bed height in the riser. Also, to simulate particle to particle interaction, it was needed to set close pack volume fraction and maximum momentum redirection. close pack volume fraction is the volume taken by number of particles in a given space of volume. close pack volume fraction parameter was set to 0.65 and maximum momentum redirection from collision was set to 40%.

2.5.6 Boundary Conditions:

After the discretization of the model into appropriate finite elements, boundary types have to be assigned to inlet and outlets of the system. there are three type of boundaries which are pressure boundaries, one injection boundary and a flow boundary. These boundary types will be discussed respectively.

2.5.6.1 Pressure Boundary Conditions:

First the air was fed from the inlet of the riser at the bottom and it was exhausted to the open air through the top. Due to the fact that air fed to a riser is released into the environment when it exits, the pressure at the outlet is equal to the pressure in the environment.

2.5.6.2 Injection Boundary Conditions:

There are two inlets to the riser. One of these inlets is the air injected in the riser.
The air enters the riser through distributer plate. During this injection no particle exits the riser.

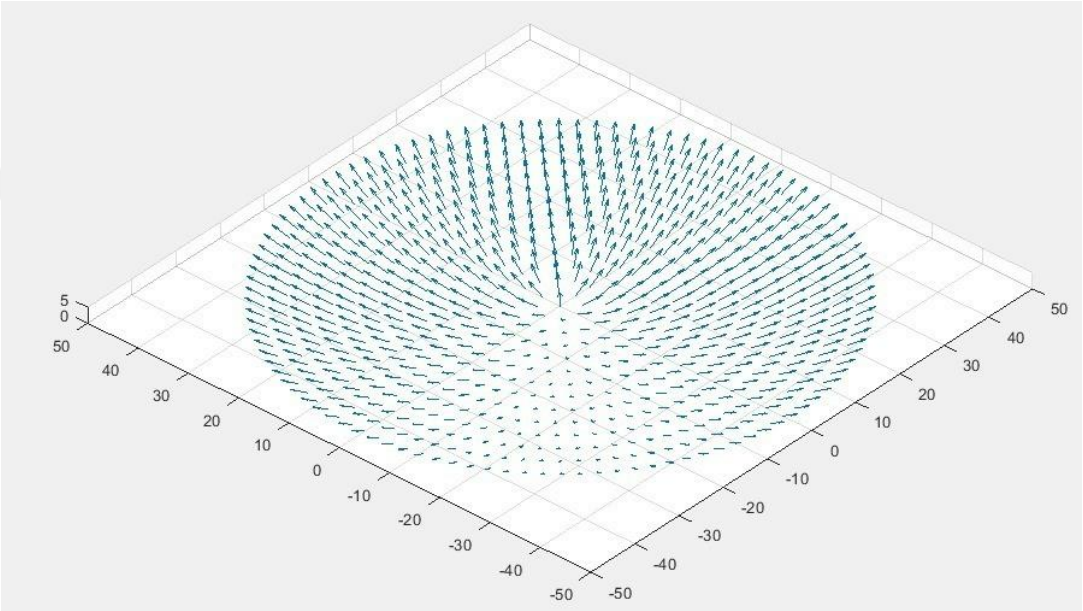

Figure 2-4 distribution plate

2.5.6.3 Flow Boundary Conditions:

A part of the air released from the top of the riser was fed from the inlet after distributer plate.

2.5.6.4 Velocity Boundary Condition Studies

Air was used for gasification agent and the flowrates of air were, 25, 32 and 38 Nm^3/h for 4, 5 and 6 m/s superficial gas velocity inside the riser.

3 RESULTS AND DISCUSSIONS

3.1 Geometrical design

Solidworks v2017 software was used for specifying the geometry (drawing). 3 dimensional was designed and imported to the Barracuda software.

3.1.1 Mesh Independency Studies

Mesh independency occurs when a given fixed type of element and free mesh, is discretized in which the solution does not depend on the size of the finite element. A uniform mesh type was used for the analysis, with 20000 elements, 40000 elements, and 80000 elements placed on the axisymmetric planes of the 3-dimensional model in order to be able to conclude that the results are independent of mesh size. Figure 3.1 depicts the riser's overall layout and construction

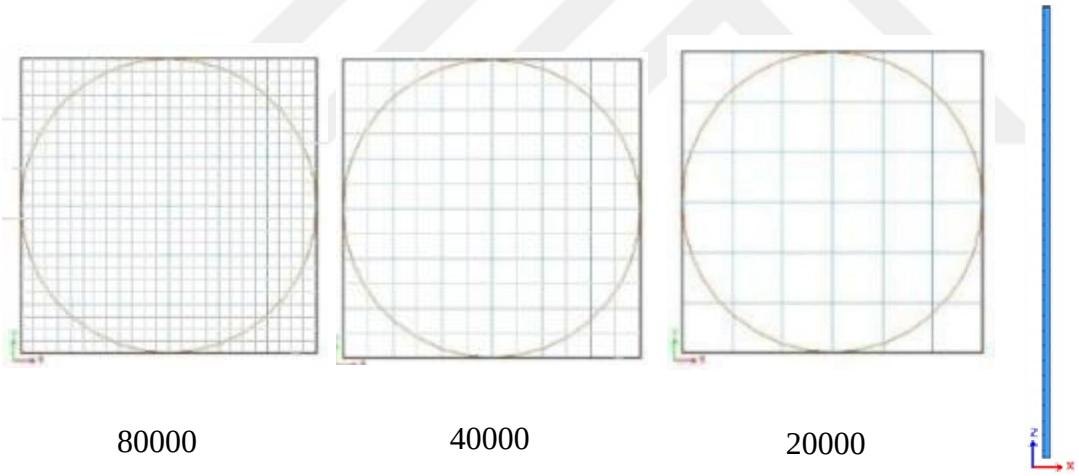

Figure 3-1 riser geometrical design with different meshing size

Because the simulation can be run using a variety of meshing sizes, we need to ensure that the outcomes are not dependent on the number of meshing that were used. In consideration of these factors, three distinct meshing cell sizes were selected (80000, 40000, 20000). The pressure results for all three meshing sizes were shown in Figure

3.2 and the error for different mesh sizes compared to experimental results are shown in table 3.1.

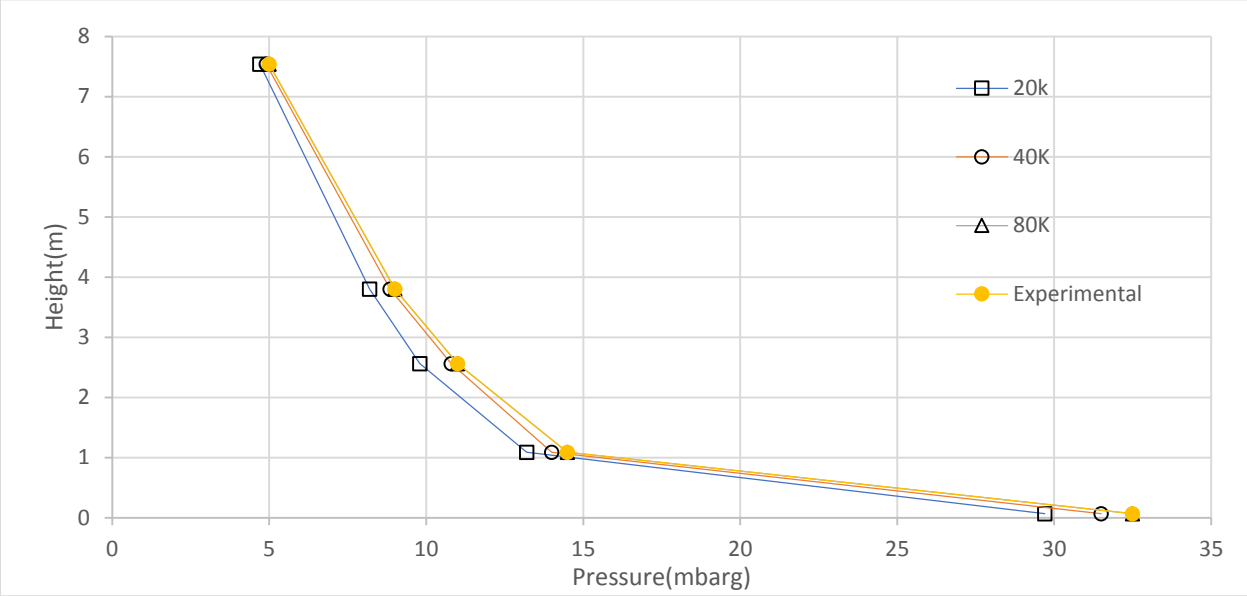

Figure 3-2 comparison of axial pressure distribution using different meshing cells

Height(m)	80K Mesh	40k Mesh	20k Mesh
0.07	0.54	3.60	9.11
1.09	0.28	3.71	9.22
2.56	1.11	2.91	11.90
3.80	0.44	2.10	9.29
7.54	0.41	1.94	7.37

As seen in table 3.1, the pressure results for all three meshing sizes converged to almost the same point. The results for 40,000 and 80,000 cells were practically equal, with error percentages of less than 5%, however, the results for 20,000 cells were slightly different, with error percentages ranging from 7% to 12%. While the results in 40k and 80k had acceptable error rates, we chose the 40k meshing size because it is time-efficient because of the lower computational load.

3.2 Numerical Studies

3.2.1 Cloud number Independency Studies

We used the Barracuda software to set the number of clouds to one of three different cloud numbers in order to demonstrate that the outcomes of our simulation are not dependent on the number of

clouds. These sizes are as follows: 3.42E+03, 7.79E+03, and 1.14E+04, respectively. The outcomes from each of these three distinct cloud numbers were compiled, and we examined and analysed them. The findings indicated that the analysis results are not dependent on the particle number because the data converged at various points throughout the riser. Figure 3.3 represents the whole set of results, and table 3.2 gives the margin of error for the results.

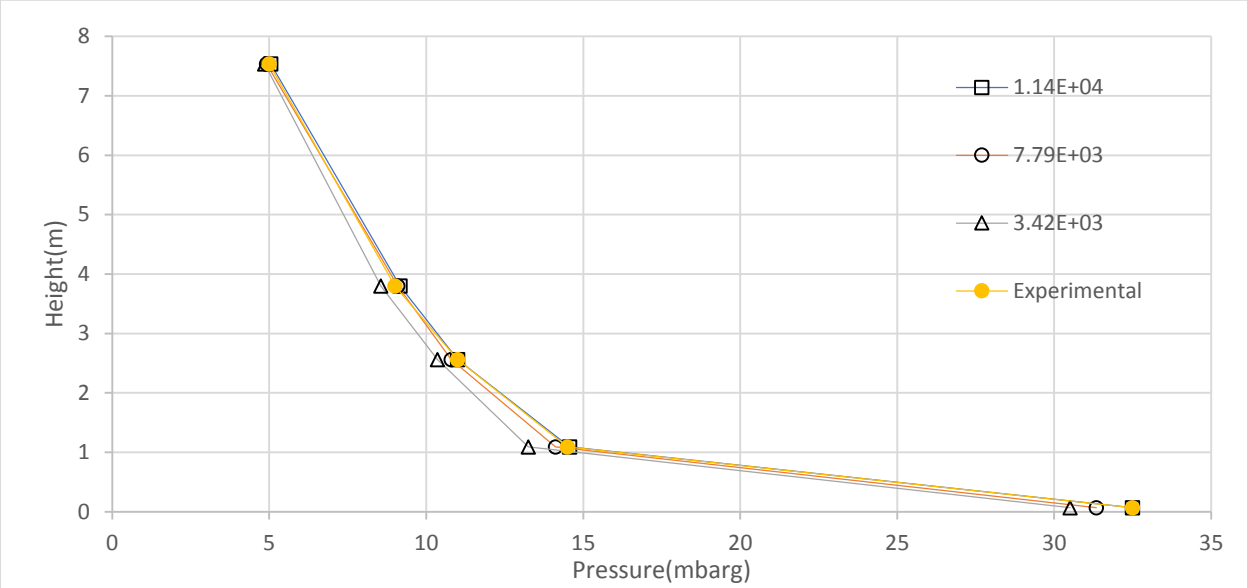

Figure 3-3 comparison of axial pressure distribution using different cloud numbers

Height(m)	(1.14E+04)	(7.79E+03)	(3.42E+03)
0.07	0.00	3.55	6.12
1.09	0.47	2.59	8.65
2.56	0.01	1.85	5.83
3.80	1.75	1.00	5.04
7.54	0.98	1.77	2.92

It is evident that the cloud number of 7.79E+03 was extremely near to the simulation with 1.14E+04 cloud numbers with an error rate of less than 4%, which is acceptable compared to the cloud number of 3.42E+03 with an error rate of 5 to 8%. As a result, the cloud number of 7.79E+03 was picked since it produced an efficient and precise outcome.

3.2.2 Effects of Drag Modelss

We simulated the riser using both the Wen-Yu Ergun and the EMMS drag models so that we could draw the conclusion that the results of the simulation are not dependent on the drag model. Both models produced results that were comparable to one another, as shown in figure 3.4 There was a marginal disparity in the results obtained by the two models up until the height of 4 metres, but after that point, the results began to converge.

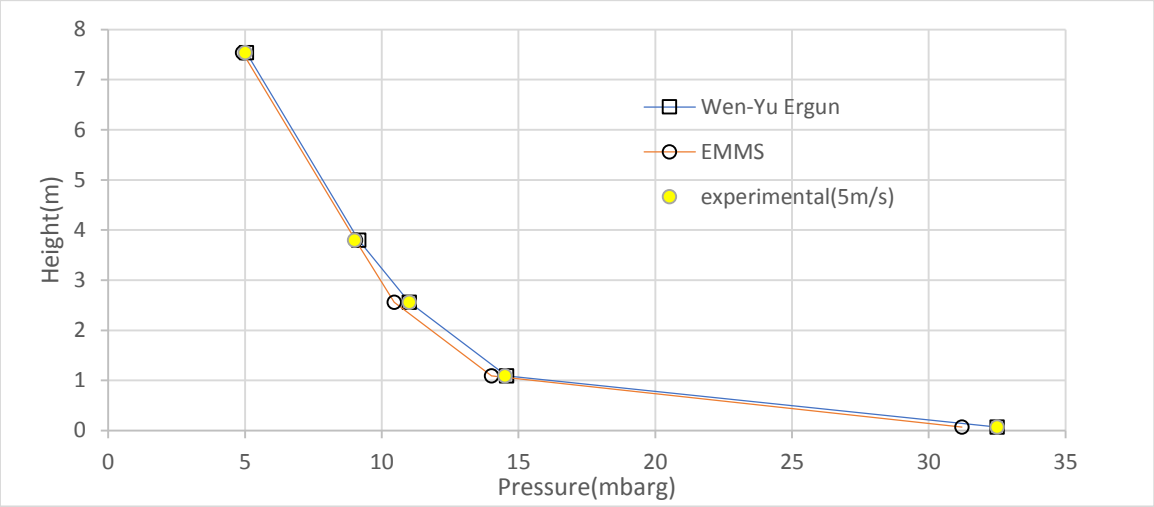

Figure 3-4 comparison of axial pressure distribution using Wen-Yu Ergun and EMMS drag models and experimental results

The error percentages for both drag models are calculated compared to experimental results and demonstrated in table 3.3.

Height(m)	Wen-Yu Ergun	EMMS
0.07	0.00	3.96
1.09	0.47	3.36
2.56	0.01	4.94
3.80	1.75	0.51
7.54	0.98	1.77

As it can be seen in table 3.3, the error for results of both drag models have error below 5% which shows the drag model independency of our simulation.

3.2.3 Air Velocity Studies and Comparison with Experimental results

In order to provide evidence that the result of the simulation can be trusted, the simulation was used to calculate the pressure at five different points along the riser by using the the pressure sensors at different heights located along the experimental riser. These simulations were carried out on three different air flow rates, each of which was 4 metres per second, 5 metres per second, and 6 metres per second using Wen-Yu Ergun drag model with 40k mesh size, in order to demonstrate that the rxperiment is independent from air velocity. We were able to perform this calculation because the experiment provided us with the necessary pressure data for the flow rates that we were interested in. The outcomes of the simulation as well as the experiments were compared, and the findings of the analysis can be seen in figures 3.5, 3.6, and 3.7.

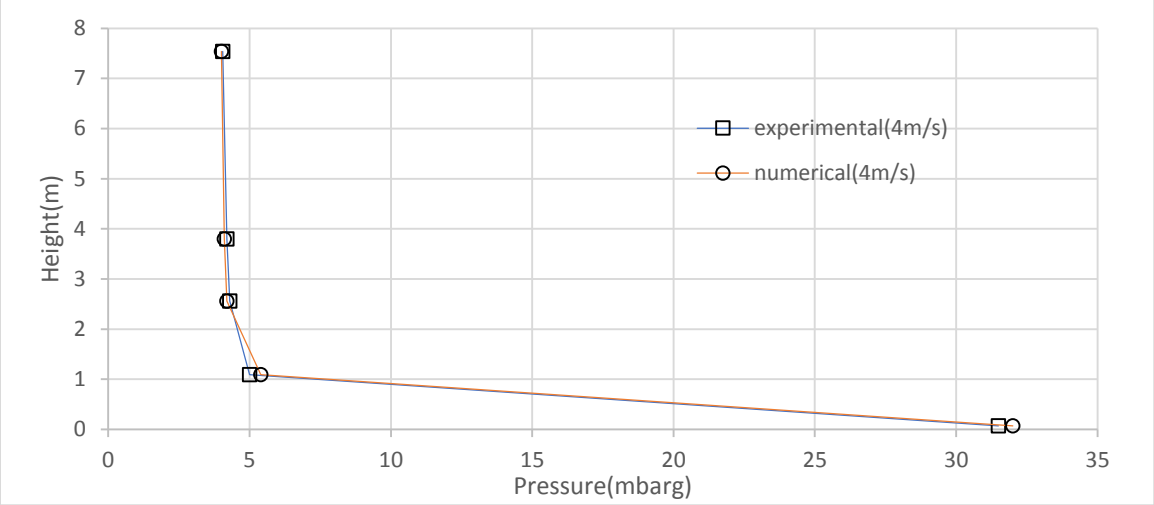

Figure 3-5 Comparison of axial pressure distribution using numerical simulation and experimental results at 4m/s

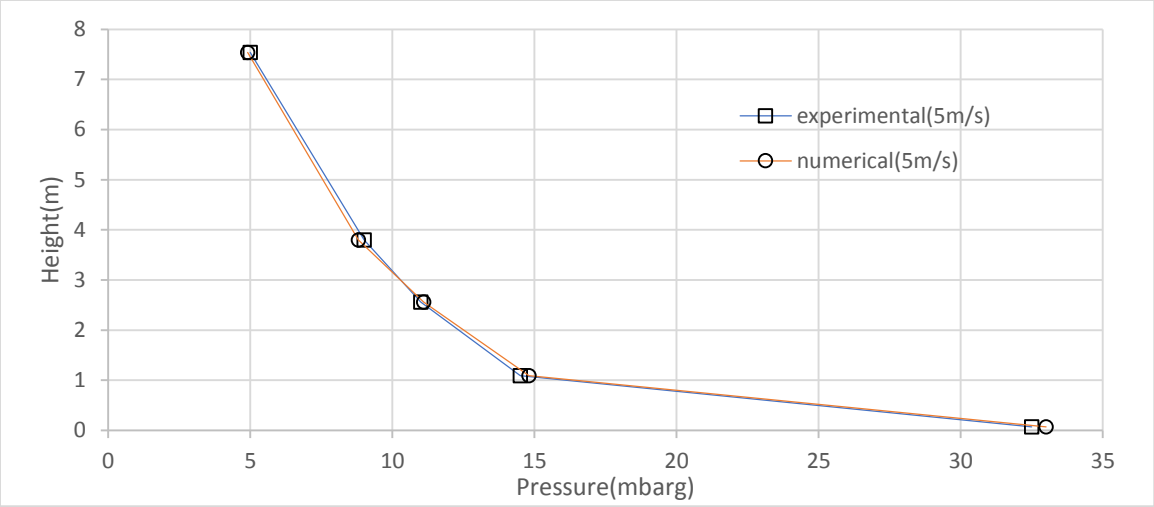

Figure 3-6 Comparison of axial pressure distribution using numerical simulation and experimental results at 5m/s

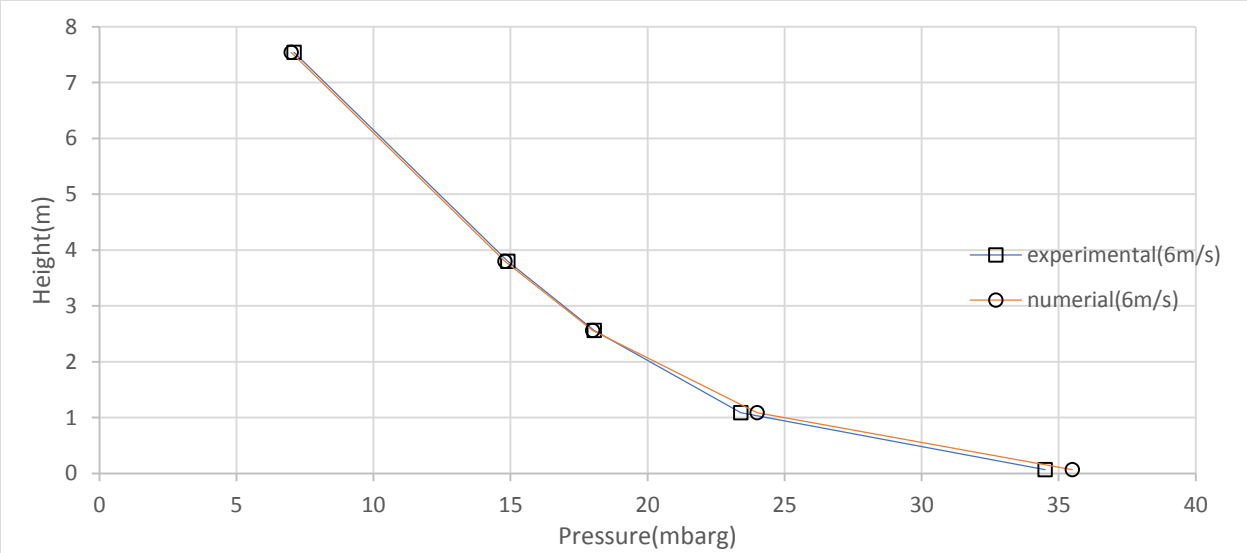

Figure 3-7 Comparison of axial pressure distribution using numerical simulation and experimental results at 6m/s

As it can be seen the results of the simulation and experiment are close and at higher heights the results converges with each other and we can see that by the increase of flowrate the pressure increases slighty. At a gas velocity of 4 m/s, the majority of the pressure drop in the riser happens within the lower 1 meter, accounting for 98% of the overall pressure drop. Additionally, most of

the bed inventory is located within this lower 1 meter, resulting in a regime that does not circulate as a fluidized bed. When comparing the solid distribution within the riser, a more uniform distribution is observed at 5 m/s and even more so at 6 m/s superficial gas velocity.

Height(m)	Numerical sim. 4m/s	Numerical sim. 5m/s	Numerical sim. 6m/s
0.07	1.59	1.54	2.90
1.09	4.50	2.07	2.60
2.56	2.33	0.91	0.30
3.80	2.38	2.22	0.70
7.54	1.23	2.00	1.40

When the errors at different flow rates are evaluated in table 3.4, it is possible to conclude that the mistakes are less than 5%, which is appropriate and valid.

Regarding the particle distribution inside the riser, the particles started out at the bottom and gradually rose to higher heights within the riser until there is a consistent, stable distribution of particles throughout the riser. The riser had a constant pressure when no air was flowing into it, but when air did, the pressure increased in stages, starting at the top and moving down until the top and bottom pressures were equal and the pressure in the middle cells was higher than the pressure in the top and bottom cells. The pressure at the bottom of the riser increased over time while the pressure at the top of the riser decreased relative to the middle cells.

3.2.4 Minimum Fluidization

Experiments and the process of modelling both used the pressure drop method in order to determine the minimum fluidization velocity[34]. This was done so that the results of each could be compared. The two approaches were evaluated side by side to achieve this result. This was done in order to ensure that a precise analysis of the results could be carried out. Wen Yu/Erun model was used during the experiment since the results were close to experminetal measurements[35].At a variety of different superficial gas velocities, the pressure drop that occurs throughout the entirety of the fluidized bed is measured. Because of this, we are able to produce a representation of the pressure drop that is more accurate and it is now possible to obtain more accurate results. During the course of the process, the velocity of the gas that is being worked with is first sped up to a higher level, and then it is slowed down to a lower level. It is essential to complete this step-in order to eliminate the possibility of encountering hysteresis. Hysteresis is typically observed as a

direct result of utilising this method, so it is important to complete this step. After that, the calculation to determine the minimum fluidization velocity can be made by using the data for the decreasing superficial gas velocity. This will allow the minimum fluidization velocity to be determined. This can be accomplished by first plotting two lines that roughly represent the pressure drop under fixed bed conditions and then fluidized bed conditions, and then locating the point at which these two lines intersect with one another. This can be done by first plotting two lines that roughly represent the pressure drop under fixed bed conditions and then fluidized bed conditions. To accomplish this, first plot two lines that roughly represent the pressure drop under fixed bed conditions, and then plot two lines that roughly represent the pressure drop under fluidized bed conditions.

When attempting to calculate an accurate minimum fluidization velocity all the way through the model, it is absolutely necessary to have a complete comprehension of the role that the close pack factor plays in the process. This is because the close pack factor plays a significant role in determining the accuracy of the minimum fluidization velocity. The amount of pressure loss that takes place in the region that is characterised by the fixed bed can be affected by the value of the close pack factor. This effect is brought about by the stationary bed. This is because the pressure loss in the region of the fluidized bed is only dependent on the weight of the suspended particle bed. This is the case because fluidization makes the bed more porous. The reasoning behind why things are the way they are can be summed up as follows: Because of the close pack factor, the pressure drop in the fixed bed will be magnified to an increasing degree as the level of the bed rises. In consequence of this, the gradient of the fixed bed line will advance toward a steeper angle, although the close pack factor will continue to be the same. This, in turn, will cause the intersection of the fixed and fluidized bed lines to shift to lower superficial gas velocities. This will occur because the superficial gas velocities will be lower. This is going to happen due to the fact that the superficial gas velocities are going to be lower. This is going to take place as a direct result of the lower superficial gas velocities that are going to be present. As a result of this reality, it has been predicted that the minimum fluidization velocity will decrease in a manner that is directly proportional to the increase in the close packing factor. This will occur as a direct consequence of the fact that the close packing factor is increasing; it is increasing at a faster rate now than it did before.

For the purpose of determining the minimum fluidization velocity, the rate of air flow had to be gradually slowed down until the particles were able to settle. Only then could the minimum fluidization velocity be calculated. After that, only then was it possible to calculate the minimum fluidization velocity. The purpose of the experiment was to find out what the minimum fluidization velocity should be, so this was done in order to accomplish that. After some deliberation, it was decided that the fluidization velocity for our simulation should be set at a level no lower than the velocity at which the air was moving at this particular point. After much thought and consideration, we came to this conclusion. In order for us to accurately determine the Reynold's number as well as the minimum fluidization velocity, we relied on two distinct formulas, one for each calculation. Both of these formulas were utilised in order to determine the Reynold's number and the minimum fluidization velocity, respectively. In the paragraphs that follow, these two equations will each be broken down in detail. The chart that was produced as a result of running the simulation can be seen in the figures 3.8 and 3.9 that can be found further down on this page.

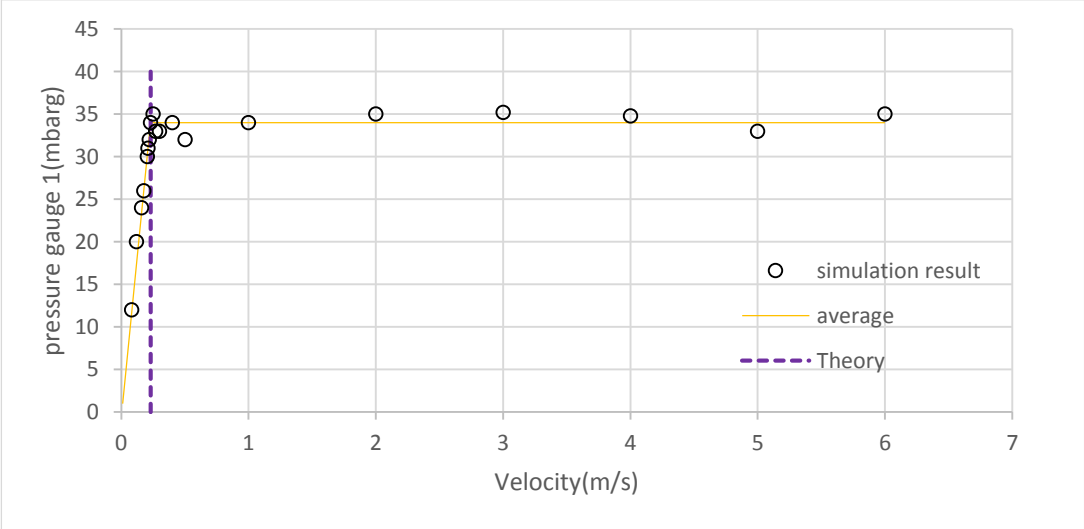

Figure 3-8 Pressure drops across the fluidized bed

Many correlations have been offered for calculating the minimal fluidization velocity. The following table lists common correlations found in publication [36] .

Table 3.5. Minimum fluidization velocity for 1, 5 and 10 bar with different Correlation

Author	Correlation	U_{mf} (1bar)	U_{mf} (5bar)	U_{mf} (10bar)
[37]	$Re_{mf} = [(33.7)^2 + 0.0408Ar]^{0.5} - 33.7$	0.23	0.136	0.127
[38]	$Re_{mf} = [(25.7)^2 + 0.0365Ar]^{0.5} - 25.7$	0.252	0.142	0.141
[39]	$Re_{mf} = [(25.3)^2 + 0.0571Ar]^{0.5} - 25.3$	0.515	0.230	0.152
[40]	$Re_{mf} = [(25.3)^2 + 0.0651Ar]^{0.5} - 25.3$	0.483	0.259	0.157
[41]	$Re_{mf} = [(27.2)^2 + 0.0408Ar]^{0.5} - 27.2$	0.285	0.158	0.144
[42]	$Re_{mf} = [(28.7)^2 + 0.0494Ar]^{0.5} - 28.7$	0.334	0.188	0.152
[43]	$Re_{mf} = [(18.7)^2 + 0.0313Ar]^{0.5} - 18.7$	0.289	0.144	0.142
[44]	$Re_{mf} = [(31.6)^2 + 0.0425Ar]^{0.5} - 31.6$	0.260	0.151	0.143

U_{mf} is calculated using the general correlation equation of

$$Re_{mf} = \frac{U_{mf} d_p \rho_g}{\mu} = [C_1^2 + C_2 Ar]^2 - C_1$$

Where C1 and C2 are empirical constants and Ar stands for Archimedes number.

The obtained minimum fluidization velocities for the tested pressure conditions at 300 K are shown in Table with various correlations.

3.2.5 Steady Behavior of simulation in high-pressure and high temperature

After ensuring that the results obtained by the simulator are accurate and reliable, a simulation was run with two distinct temperatures, three distinct pressures, and a flowrate of six meters per second. The temperature and pressures of the atmosphere increased, which led to an increase in the pressure difference between the riser's internal pressure and that of the atmosphere. In addition to this, the differential in pressure increased at the same time as the temperature climbed as well. As illustrated in Figure 3.10, pressure differences increase as pressure increases. The pressure differential was greater than 5bar in 10bar and greater than 1bar in 5bar.

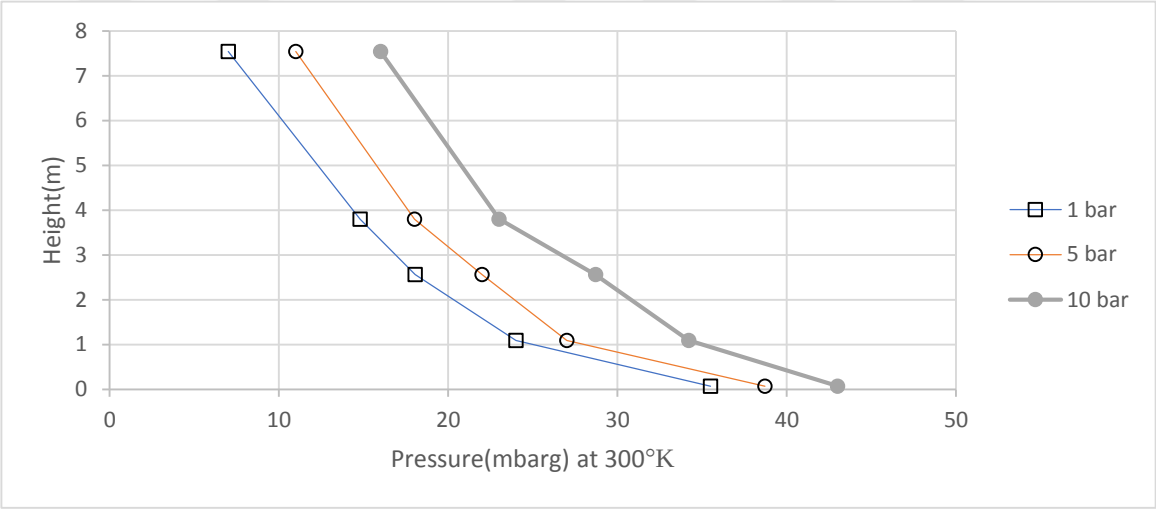

Figure 3-9 Comparison of axial pressure distribution at 6m/s and 300°K in in 1, 5 and 10 bar.

The same thing can be seen in the figure 3.11, and the same pattern can be seen once the temperature is set to 300°K.

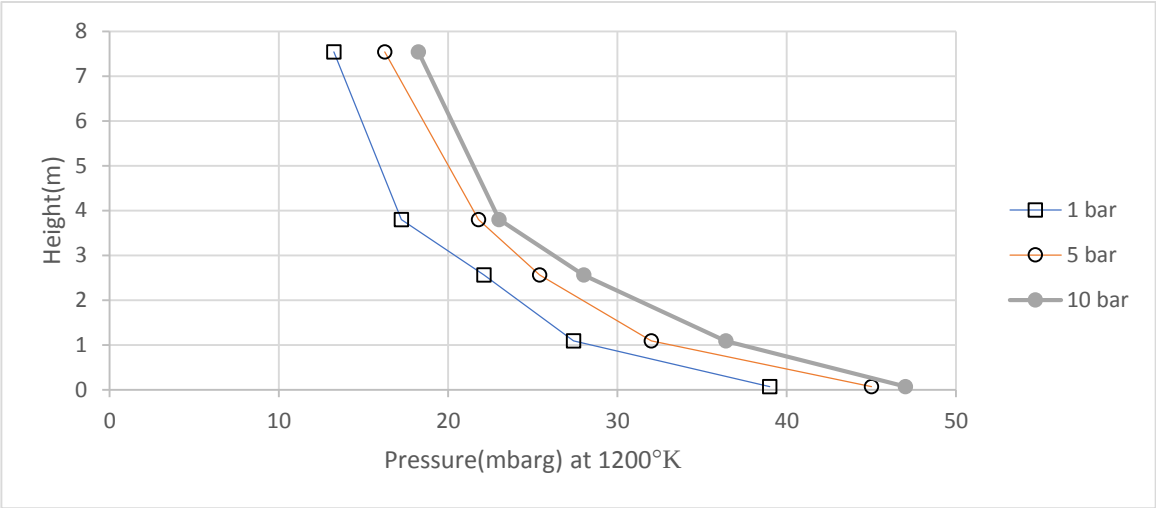

Figure 3-10 Comparison of axial pressure distribution at 6m/s and 1200°K in in 1, 5 and 10 bar.

The figure 3.11 that is displayed above shows the changes in pressure that occur at three different pressures when the temperature is 1200 degrees Kelvin. The pressure differences also rose as the pressure continued to climb.

3.2.6 Riser Simulation results

The results for particle distribution and pressure all over the riser through time in the conducted simulation are shown below.

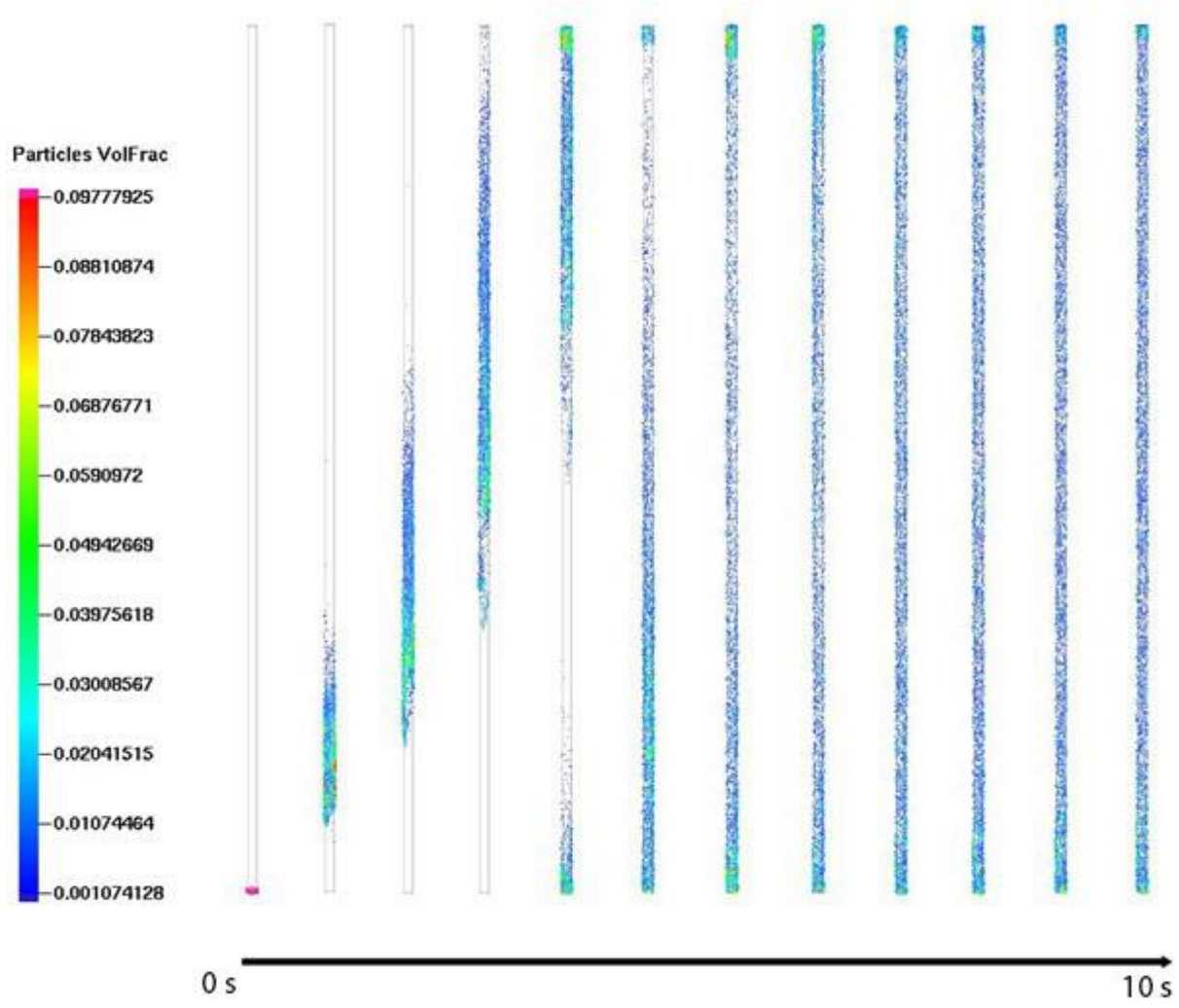

Figure 3-11 Particle distribution inside riser through time since the start of air flow

As can be seen in the figure 3.12 , the particles were initially positioned at the bottom of the riser and gradually rose to higher heights within the riser until there is a uniform stable distribution of particles all over the riser.

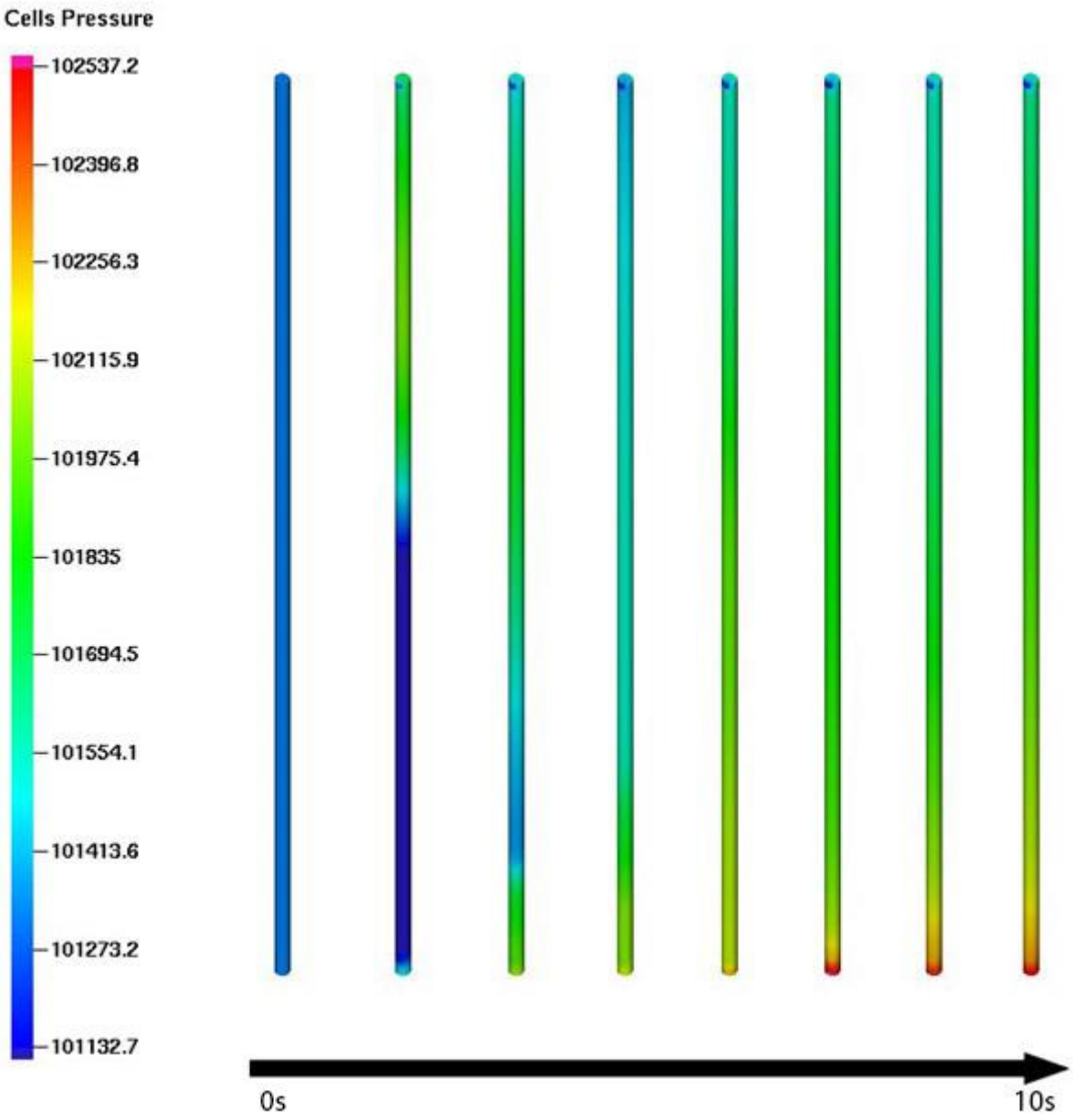

Figure 3-12 Pressure of the cells inside riser through time since the start of air flow

As can be seen in figure 3.13, when no air flowed into the riser, the pressure throughout the riser was the same, and when air flowed into it, the pressure at the top of the riser increased first, followed by the pressure at the lower heights, until the pressure at the top and bottom of the riser were the same, and the pressure in the middle cells was higher than the pressure at the top and

bottom. In comparison to the middle cells, the pressure at the lower end of the riser increased over time, while the pressure at the top end decreased.

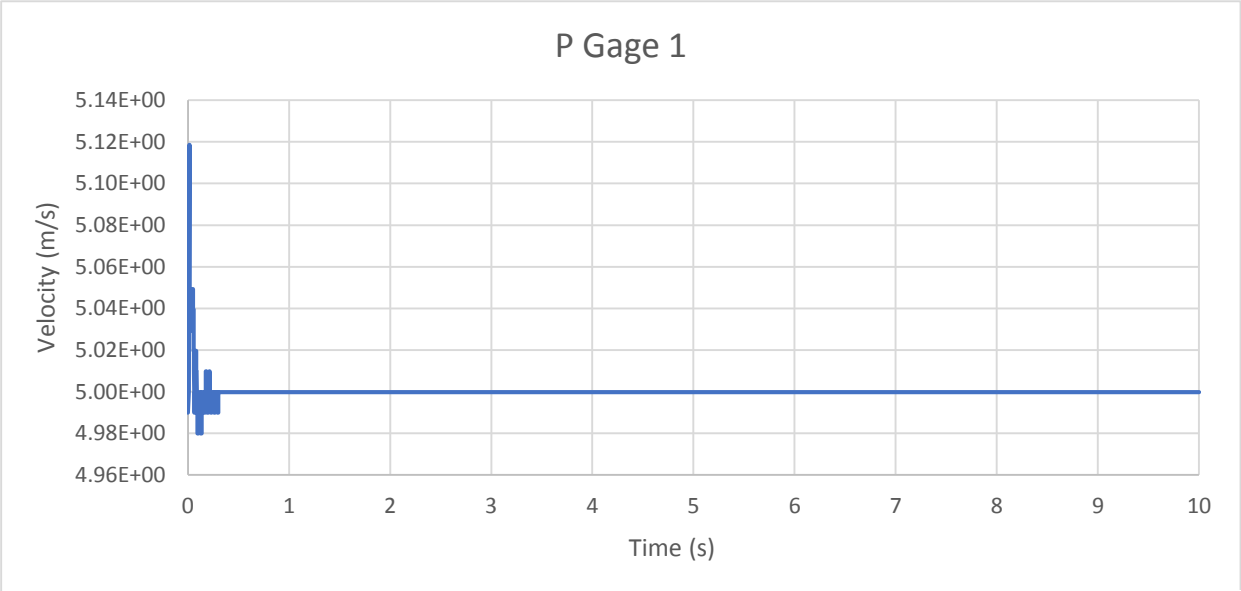

Figure 3-13 Pressure of the Gage 1 insdie riser through time since the start of air flow

An instance of simulations presented in figure 3-14 indicates that the pressures remain constant after a few seconds. However, to ensure the accuracy of the findings, we extended the calculations up to 10 seconds.

4 CONCLUSION

The numerical studies of a circulating fluidized bed chamber under pressurised conditions were conducted as the scope of the thesis. The axial pressure distributions along the CFB reactor have been obtained at different operating conditions. The numerical results were compared to the outcomes of the previous experiments that had been carried out on a laboratory scale CFB test setup located at TUBITAK MRC premises.

Barracuda Virtual Reactor® v17.4.0 software has been used in simulations. The mesh independence study has been carried out to show that the simulation results are independent of the mesh numbers. According to the research conducted, a mesh of 40k was found sufficient enough to achieve accurate results. All three meshing sizes produced almost at similar pressure results with error rate of almost 10%. However, because the deviation of 20K cell results was more(7%~12%) than 40K and 80K(less than 5%), and the simulation time of 80K was longer, 40K cell size was decided to be used in further simulations because it was accurate enough and needed less simulation time.

Additionally, the simulations have been carried out for three different cloud numbers, and the findings have been compared. It was found that 7.79E+03 number of clouds is enough and used in the further parametric simulations.

The riser was simulated using the Wen-Yu Ergun and EMMS drag models to examine which drag model better predicts the axial pressure distribution. Both models produced similar results with error rate less than 5% compared to experiments. On the other hand, Wen-Yu Ergun model predicted better the results with an error rate below 2% compared to measurements. Therefore, this model has been chosen for further analysis. The simulation was performed to compare the pressure results at five different points along the riser with experimental measurements conducted by using the pressure sensors. The simulations were realized at 4 m/s, 5 m/s, and 6 m/s gas velocities using Wen-Yu Ergun drag model with 40k mesh size to investigate the pressure distribution along the riser by varying the air flow velocity.

The superficial gas velocity has been changed to calculate the minimum fluidization velocity by drawing a diagram for pressure drop versus air velocity. At the end of the simulations the error

rate for pressure values at all three flow rates were below 5%. To determine the minimum fluidization velocity, the air flow rate had to be slowed down until particles settled. This study was performed to determine the minimum fluidization velocity. Various correlations from the literature were employed to carry out the theoretical calculation of the minimum fluidization velocity. The corrleation developed by Wen, C. Y. and Yu, Y. H. in the first row of Table 3.5 predicted closer the minimum fludization velocity compared to numerical findings.

Increasing pressure leads to a corresponding increase in pressure along the riser, as observed at 1, 5, and 10 bar. The behavior of pressure remains consistent when the temperature is increased from 300K to 1200K. However, the data also suggests that other factors can impact this relationship, as increasing pressure at 300K for 10 bar results in a greater change in pressure along the riser than increasing pressure at 1200K for 10 bar. Further research is needed to better understand the complex interplay between pressure and temperature in the riser of the CFB reactor.

In conclusion, we were able to simulate the riser of a CFB bed and the results were reliable. It can be concluded that the obtained simulation data satisfied our expectation and showed that simulations can predict accurate enough the hydrodynamics of the flow developed in the fluidized bed system and can be used in design of fluidized bed reactors before construction and evaluation of the possible problems.

REFERENCES

[1] Energy Statistics Division of the International Energy Agency, (2011), Key World Energy Statistic Report.

[2] International Energy Agency, (2009), Energy Balance for World, http://www.iea.org/stats/balancetable.

[3] Republic Of Turkey Ministry of Energy and Natural Resources, (2009), Energy Balance For Turkey.

[4] Conti, J., Holtberg, P., (2011), International Energy Outlook 2011, U.S. Energy Information Administration.

[5] Turkish Coal Enterprises, (2009), Coal Sector Report (Lignite).

[6] Balat, M., (2005), Use of biomass sources for energy in Turkey and a view to biomass potential, Biomass and Bioenergy 29, 32-41.

[7] Oka, Simeon. Fluidized bed combustion. CRC press, 2003.

[8] Gupta, . "Some Advanced Application Areas of Fluidization", Fluid Bed Technology in Materials Processing, 1998

[9] U.S. Department Of Energy, National Energy Technology Laboratory, (2010), Gasification 2010 Worldwide Database.

[10] U.S. Energy Information Administration, (2009), International Energy Statistics.

[11] Everitt, E., (2007), Gasification and IGCC: Status and Readiness, Wyoming Coal Gasification Symposium, 2007, Wyoming.

[12] Anthony, E. J. "Fluidized bed combustion of alternative solid fuels; status, successes and problems of the technology." Progress in Energy and Combustion Science 21.3 (1995): 239-268.

[13] Joris Koornneef, Martin Junginger, André Faaij, Development of fluidized bed combustion—An overview of trends, performance and cost, Progress in Energy and Combustion Science, Volume 33, Issue 1, 2007, Pages 19-55, ISSN 0360-1285, https://doi.org/10.1016/j.pecs.2006.07.001.

[14] P. Basu, Combustion and Gasification in Fluidized Beds, vol. 53, no. 9. 1981.

[15] Basu, . "Characteristics of Solid Particles", Combustion and Gasification in Fluidized Beds, 2006

[16] J. Koornneef, M. Junginger, and A. Faaij, “Development of fluidized bed combustion-An overview of trends, performance and cost,” Prog. Energy

[17] https://dokumen.tips/documents/iea-fluidized-bed-conversion-programme.html

[18] Al-Agili, Zahraa. (2007). Mass Transfer of Naphthalene from an Immersed Surface to a Sand_air Fluidized Bed. 10.13140/RG.2.2.21092.71040.

[19] Yates, J.G., Lettieri, P. (2016). Introduction. In: Fluidized-Bed Reactors: Processes and Operating Conditions. Particle Technology Series, vol 26. Springer, Cham. https://doi.org/10.1007/978-3-319-39593-7_1

[20] https://en.wikipedia.org/wiki/Fluidized_bed_combustion

[21] Adamczyk, Wojciech. (2016). Application of the Numerical Techniques for Modelling Fluidization Process Within Industrial Scale Boilers. Archives of Computational Methods in Engineering. 24. 10.1007/s11831-016-9186-z.

[22] Snider, D. M.; Clark, S. M.; O’Rourke, P. J. 2011, "Eulerian–Lagrangian method for threedimensional thermal reacting flow with application to coal gasifiers", Chemical Engineering Science, Vol. 66, No. 6, 1285–1295. doi:10.1016/J.CES.2010.12.042

[23] Anderson, T. B.; Jackson, R. 1967, "Fluid mechanical description of fluidized beds: Equations of Motion", Industrial and Engineering Chemistry Fundamentals, Vol. 6, No. 4, 527–539. doi:10.1021/i160024a007

[24] Snider, D. M. 2001, "An Incompressible Three-Dimensional Multiphase Particle-in-Cell Model for Dense Particle Flows", Journal of Computational Physics, Vol. 170, No. 2, 523–549. doi:10.1006/JCPH.2001.6747

[25] Harris, S. E.; Crighton, D. G. 1994, "Solitons, Solitary Waves, and Voidage Disturbances in Gas-Fluidized Beds", Journal of Fluid Mechanics, Vol. 266, 243–276. doi:10.1017/S0022112094000996

[26] M. Dianat, Z. Yang, J.J. McGuirk, Large Eddy Simulation of Scalar Mixing, Editor(s): W. Rodi, M. Mulas, Engineering Turbulence Modelling and Experiments 6, Elsevier Science B.V., 2005, Pages 823-832, ISBN 9780080445441, https://doi.org/10.1016/B978-008044544-1/50079-0.

[27] Wang, Meng & Moin, Parviz. (2002). Dynamic wall modeling for large-eddy simulation of complex turbulent flows. Physics of Fluids - PHYS FLUIDS. 14. 10.1063/1.1476668.

[28] Saurabh Gupta, Shikhar Choudhary, Suraj Kumar, Santanu De, Large eddy simulation of biomass gasification in a bubbling fluidized bed based on the multiphase particle-in-cell method, Renewable Energy, Volume 163, 2021, Pages 1455-1466, ISSN 0960-1481, https://doi.org/10.1016/j.renene.2020.07.127.

[29] Ergun, S. (1952) Fluid Flow through Packed Columns. Chemical Engineering Progress, 48, 89-94.

[30] Wen, C.Y. and Yu, Y.H. (1966) Mechanics of Fluidization

[31] Krishnadash S. Kshetrimayum, Seongho Park, Chonghun Han, Chul-Jin Lee, EMMS drag model for simulating a gas–solid fluidized bed of geldart B particles: Effect of bed model parameters and polydisperity, Particuology, Volume 51, 2020, Pages 142-154, ISSN 1674-2001, https://doi.org/10.1016/j.partic.2019.10.004.

[32] Serhat Gül , 2016, " Experimental and Theoretical Investigation of Fluidized Bed Gasification with Cold and Hot" PhD Thesis, Marmara University.

[33] Geldart,D."Types of Gas Fluidization," Powder Technology, 7, pp. 285-292 (1972).

[34] Wen, C. Y., and Y. H. Yu, " A Generalized Method for Predicting the Minimum Fluidization Velocity," AIChE Journal, 12, pp. 610-612 (1966).

[35] Öner, B.A., Bektaş, Z. and Yılmaz, B., 2023. Numerical Analysis and Experimental Verification on Flow Characteristics of a Pressurized Fluidized Bed System. Journal of Energy Resources Technology, 145(3), p.031703.

[36] Li, L.; Duan, Y.; Duan, L.; Xu, C.; Anthony, E. J. 2018, "Flow characteristics in pressurized oxy-fuel fluidized bed under hot condition", International Journal of Multiphase Flow, Vol. 108, 1–10. doi:10.1016/j.ijmultiphaseflow.2018.06.020

[37] Wen, C. Y.; Yu, Y. H. 1966, "A Generalized Method for Predicting the Minimum Fluidization Velocity", 610–612

[38] Couderc, J. P. 1985, "Incipient fluidization and particulate systems".

[39] Saxena, S. C.; Vogel, G. J. 1977, "Measurement of Incipient Fluidisation Velocities in a Bed of Coarse Dolomite at Temperature and Pressure"., Trans Inst Chem Eng, Vol. 55, No. 3

[40] Babu, S. P.; Shah, B.; Talwalkar, A. 1978, "Fluidization Correlations for Coal Gasification Materials - Minimum Fluidization Velocity and Fluidized Bed Expansion Ratio"., AIChE Symp Ser (Vol. 74)

[41] Grace, J. B. 1983, "Hydrodynamics of liquid drops in immiscible liquids".

[42] Kornosky, R. M. 1983, "Characteristics of fluidization at high pressure"

[43] Zheng, Y.; U, J. J. Z. H.; Wen, J.; Martin, S. A.; Amarjeet, S. 1999, "The Axial Hydrodynamic Behavior in a LiquidSolid - Circulating Fluidized Bed", Vol. 77

[44] Thonglimp, V.; Laguerie, N. H. C. 1981, "Vitesse UnGaZ Minimale de Fluidisation et Expansion des Couches Fluidisks", par, Vol. 38, 233–253

REFERENCES

[1] Energy Statistics Division of the International Energy Agency, (2011), Key World Energy Statistic Report.

[2] International Energy Agency, (2009), Energy Balance for World, http://www.iea.org/stats/balancetable.

[3] Republic Of Turkey Ministry of Energy and Natural Resources, (2009), Energy Balance For Turkey.

[4] Conti, J., Holtberg, P., (2011), International Energy Outlook 2011, U.S. Energy Information Administration.

[5] Turkish Coal Enterprises, (2009), Coal Sector Report (Lignite).

[6] Balat, M., (2005), Use of biomass sources for energy in Turkey and a view to biomass potential, Biomass and Bioenergy 29, 32-41.

[7] Oka, Simeon. Fluidized bed combustion. CRC press, 2003.

[8] Gupta, . "Some Advanced Application Areas of Fluidization", Fluid Bed Technology in Materials Processing, 1998

[9] U.S. Department Of Energy, National Energy Technology Laboratory, (2010), Gasification 2010 Worldwide Database.

[10] U.S. Energy Information Administration, (2009), International Energy Statistics.

[11] Everitt, E., (2007), Gasification and IGCC: Status and Readiness, Wyoming Coal Gasification Symposium, 2007, Wyoming.

[12] Anthony, E. J. "Fluidized bed combustion of alternative solid fuels; status, successes and problems of the technology." Progress in Energy and Combustion Science 21.3 (1995): 239-268.

[13] Joris Koornneef, Martin Junginger, André Faaij, Development of fluidized bed combustion—An overview of trends, performance and cost, Progress in Energy and Combustion Science, Volume 33, Issue 1, 2007, Pages 19-55, ISSN 0360-1285, https://doi.org/10.1016/j.pecs.2006.07.001.

[14] P. Basu, Combustion and Gasification in Fluidized Beds, vol. 53, no. 9. 1981.

[15] Basu, . "Characteristics of Solid Particles", Combustion and Gasification in Fluidized Beds, 2006

[16] J. Koornneef, M. Junginger, and A. Faaij, “Development of fluidized bed combustion-An overview of trends, performance and cost,” Prog. Energy

[17] https://dokumen.tips/documents/iea-fluidized-bed-conversion-programme.html

[18] Al-Agili, Zahraa. (2007). Mass Transfer of Naphthalene from an Immersed Surface to a Sand_air Fluidized Bed. 10.13140/RG.2.2.21092.71040.

[19] Yates, J.G., Lettieri, P. (2016). Introduction. In: Fluidized-Bed Reactors: Processes and Operating Conditions. Particle Technology Series, vol 26. Springer, Cham. https://doi.org/10.1007/978-3-319-39593-7_1

[20] https://en.wikipedia.org/wiki/Fluidized_bed_combustion

[21] Adamczyk, Wojciech. (2016). Application of the Numerical Techniques for Modelling Fluidization Process Within Industrial Scale Boilers. Archives of Computational Methods in Engineering. 24. 10.1007/s11831-016-9186-z.

[22] Snider, D. M.; Clark, S. M.; O’Rourke, P. J. 2011, "Eulerian–Lagrangian method for threedimensional thermal reacting flow with application to coal gasifiers", Chemical Engineering Science, Vol. 66, No. 6, 1285–1295. doi:10.1016/J.CES.2010.12.042

[23] Anderson, T. B.; Jackson, R. 1967, "Fluid mechanical description of fluidized beds: Equations of Motion", Industrial and Engineering Chemistry Fundamentals, Vol. 6, No. 4, 527–539. doi:10.1021/i160024a007

[24] Snider, D. M. 2001, "An Incompressible Three-Dimensional Multiphase Particle-in-Cell Model for Dense Particle Flows", Journal of Computational Physics, Vol. 170, No. 2, 523–549. doi:10.1006/JCPH.2001.6747

[25] Harris, S. E.; Crighton, D. G. 1994, "Solitons, Solitary Waves, and Voidage Disturbances in Gas-Fluidized Beds", Journal of Fluid Mechanics, Vol. 266, 243–276. doi:10.1017/S0022112094000996

[26] M. Dianat, Z. Yang, J.J. McGuirk, Large Eddy Simulation of Scalar Mixing, Editor(s): W. Rodi, M. Mulas, Engineering Turbulence Modelling and Experiments 6, Elsevier Science B.V., 2005, Pages 823-832, ISBN 9780080445441, https://doi.org/10.1016/B978-008044544-1/50079-0.

[27] Wang, Meng & Moin, Parviz. (2002). Dynamic wall modeling for large-eddy simulation of complex turbulent flows. Physics of Fluids - PHYS FLUIDS. 14. 10.1063/1.1476668.

[28] Saurabh Gupta, Shikhar Choudhary, Suraj Kumar, Santanu De, Large eddy simulation of biomass gasification in a bubbling fluidized bed based on the multiphase particle-in-cell method, Renewable Energy, Volume 163, 2021, Pages 1455-1466, ISSN 0960-1481, https://doi.org/10.1016/j.renene.2020.07.127.

[29] Ergun, S. (1952) Fluid Flow through Packed Columns. Chemical Engineering Progress, 48, 89-94.

[30] Wen, C.Y. and Yu, Y.H. (1966) Mechanics of Fluidization

[31] Krishnadash S. Kshetrimayum, Seongho Park, Chonghun Han, Chul-Jin Lee, EMMS drag model for simulating a gas–solid fluidized bed of geldart B particles: Effect of bed model parameters and polydisperity, Particuology, Volume 51, 2020, Pages 142-154, ISSN 1674-2001, https://doi.org/10.1016/j.partic.2019.10.004.

[32] Serhat Gül , 2016, " Experimental and Theoretical Investigation of Fluidized Bed Gasification with Cold and Hot"

[33] Geldart,D."Types of Gas Fluidization," Powder Technology, 7, pp. 285-292 (1972).

[34] Wen, C. Y., and Y. H. Yu, " A Generalized Method for Predicting the Minimum Fluidization Velocity," AIChE Journal, 12, pp. 610-612 (1966).

[35] Öner, B.A., Bektaş, Z. and Yılmaz, B., 2023. Numerical Analysis and Experimental Verification on Flow Characteristics of a Pressurized Fluidized Bed System. Journal of Energy Resources Technology, 145(3), p.031703.

[36] Li, L.; Duan, Y.; Duan, L.; Xu, C.; Anthony, E. J. 2018, "Flow characteristics in pressurized oxy-fuel fluidized bed under hot condition", International Journal of Multiphase Flow, Vol. 108, 1–10. doi:10.1016/j.ijmultiphaseflow.2018.06.020

[37] Wen, C. Y.; Yu, Y. H. 1966, "A Generalized Method for Predicting the Minimum Fluidization Velocity", 610–612

[38] Couderc, J. P. 1985, "Incipient fluidization and particulate systems".

[39] Saxena, S. C.; Vogel, G. J. 1977, "Measurement of Incipient Fluidisation Velocities in a Bed of Coarse Dolomite at Temperature and Pressure"., Trans Inst Chem Eng, Vol. 55, No. 3

[40] Babu, S. P.; Shah, B.; Talwalkar, A. 1978, "Fluidization Correlations for Coal Gasification Materials - Minimum Fluidization Velocity and Fluidized Bed Expansion Ratio"., AIChE Symp Ser (Vol. 74)

[41] Grace, J. B. 1983, "Hydrodynamics of liquid drops in immiscible liquids".

[42] Kornosky, R. M. 1983, "Characteristics of fluidization at high pressure"

[43] Zheng, Y.; U, J. J. Z. H.; Wen, J.; Martin, S. A.; Amarjeet, S. 1999, "The Axial Hydrodynamic Behavior in a LiquidSolid - Circulating Fluidized Bed", Vol. 77

[44] Thonglimp, V.; Laguerie, N. H. C. 1981, "Vitesse UnGaZ Minimale de Fluidisation et Expansion des Couches Fluidisks", par, Vol. 38, 233–253